

DESIGN AND ANALYSIS OF HEPTAGONAL, OCTAGONAL, AND SPIDER-WEB PHOTONIC CRYSTAL FIBRE IN THE TERAHERTZ REGIME

A DISSERTATION

SUBMITTED IN PARTIAL FULFILLMENT OF THE REQUIREMENT FOR
THE AWARD OF THE DEGREE
OF

MASTER OF SCIENCE
IN
PHYSICS

Submitted by:

GURMEET SINGH | 2K21/MSCPHY/15
SHUBHAM SHARMA | 2K21/MSCPHY/45

Under the supervision of

Dr AJEET KUMAR
Assistant Professor



DEPARTMENT OF APPLIED PHYSICS
DELHI TECHNOLOGICAL UNIVERSITY
(Formerly Delhi College of Engineering)
Bawana Road, Delhi 110042

MAY, 2023

DEPARTMENT OF APPLIED PHYSICS
DELHI TECHNOLOGICAL UNIVERSITY
(Formerly Delhi College of Engineering)
Bawana Road, Delhi 110042

CANDIDATES' DECLARATION

We, Gurmeet Singh | 2K21/MSCPHY/15 & Shubham Sharma | 2K21/MSCPHY/45 students of M.Sc. Physics hereby declares that the project Dissertation titled “**Design and Analysis of Heptagonal, Octagonal, and Spider-Web Photonic Crystal Fibre in the Terahertz Regime**”, which is submitted by us to the Department of Applied Physics, Delhi Technological University, Delhi, in partial fulfilment of the requirement for the award of the degree of Master of Science is original and not copied from any source without proper citation. This work has not previously formed the basis for awarding any Degree, Diploma Associateship, Fellowship or other similar title or recognition. The following works have been communicated in peer-reviewed Scopus Indexed and SCImago Conferences and Journal:

1. **Title:** Analysing the Performance of Heptagonal Photonic Crystal Fibre in Terahertz Wave Propagation.
Author(s): Gurmeet Singh, Shubham Sharma, and Ajeet Kumar
Conference: International Conference on Design and Materials (ICDM) – 2023
Date & Venue: July 28-29, 2023; Delhi Technological University, Delhi, India
Paper Status: Accepted
Registered: Yes
Publish in: Journal of Mines, Metals & Fuels (Scopus Indexed)
Remarks: The paper has been accepted for publication in a journal.

2. **Title:** Design and Simulation of Solid–Core Octagonal Photonic Crystal Fibre for Terahertz Wave Propagation.
Author(s): Gurmeet Singh, Shubham Sharma, and Ajeet Kumar
Conference: Photonics 2023

Date & Venue: July 5-8, 2023; J. N. Tata Auditorium, Indian Institute of Science, Bengaluru, Karnataka, India

Paper Status: Communicated

Registered: -

Publish in: Lecture Notes in Electrical Engineering, Springer Conference Proceedings (SCI and Scopus Indexed)

Remarks: The paper is yet to be published.

3. Title: Design and Analysis of Spider-Web Photonic Crystal Fibre in the Terahertz Regime.

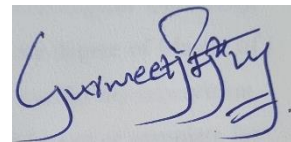
Author(s): Gurmeet Singh, Shubham Sharma, and Ajeet Kumar

Journal: The European Physical Journal D (SCI and Scopus)

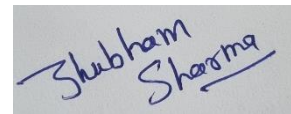
Paper Status: Communicated

Place: Delhi

Date: May 31, 2023



GURMEET SINGH



SHUBHAM SHARMA

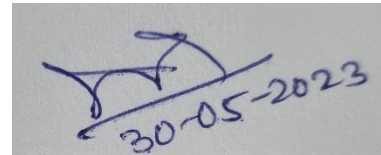
DEPARTMENT OF APPLIED PHYSICS
DELHI TECHNOLOGICAL UNIVERSITY
(Formerly Delhi College of Engineering)
Bawana Road, Delhi 110042

CERTIFICATE

I hereby certify that the project Dissertation titled “**Design and Analysis of Heptagonal, Octagonal, and Spider-Web Photonic Crystal Fibre in the Terahertz Regime,**” which is submitted by Gurmeet Singh | 2K21/MSCPHY/15 & Shubham Sharma | 2K21/MSCPHY/45, Department of Applied Physics, Delhi Technological University, Delhi, in partial fulfilment of the requirement for the award of the degree of Master of Science, is a record of the project work carried out by the students under my supervision. To the best of my knowledge, this work has not been submitted in part or complete for any Degree or Diploma to this University or elsewhere.

Place: Delhi

Date: May 31, 2023

A rectangular box containing a handwritten signature in blue ink and the date '30-05-2023' written below it.

Dr AJEET KUMAR
(Assistant Professor)

ACKNOWLEDGEMENT

Remembering the Almighty God,

We want to thank our Supervisor, Dr AJEET KUMAR, who made this work possible. His guidance and advice carried us through all stages of this research on photonic crystal fibres. We thank our Head of the Department, Prof A.S. RAO, HOD, Department of Applied Physics, for providing the facility to conduct this research. We also thank our committee members for their invaluable input and suggestions.

We are grateful to Delhi Technological University for providing us with the opportunity to conduct our research and for all the resources and support they provided. We also thank I-Stem, who provided the COMSOL Multiphysics Software license.

We would also like to thank our friends and families for their love and support during this process. Without them, this journey would not have been possible.

Finally, we would like to extend our sincere gratitude to all the participants in this study. Their willingness to share their experiences and insights has been invaluable to our research and helped to make this thesis successful. Thank you for your time and contribution.

ABSTRACT

This work proposes multiple photonic crystal fibre (PCF) designs of Heptagonal, Octagonal, and Spider-Web claddings. All designs are simulated in the COMSOL Multiphysics software using the finite element method (FEM) from the computational electrodynamics. To understand the behaviour of proposed designs in Terahertz (THz) wave transmission, the core material is infused with polymers such as Teflon, chalcogens such as chalcogenide glass, or fused silica. From the perfectly matched layer, a numerical approximation, two optical losses, a very low confinement loss, and effective material loss (EML), including other optical properties that explain the behaviour of fibre, effective mode area, nonlinearity coefficient, numerical aperture, power fraction, and V-parameter, have been reported with varying frequency from $0.1 THz$ to $4.0 THz$. By comparing all the results, these PCF designs in the fundamental mode can be used in various applications such as broadband transmission, biosensing, chemical sensing, and other THz applications.

CONTENTS

Candidates' Declaration	ii
Certificate	iv
Acknowledgement	v
Abstract	vi
Contents	vii
List of Figures	ix
List of Tables	x
List of Abbreviations/Symbols	xi
CHAPTER 1 Introduction	1
1.1 ELECTROMAGNETIC WAVES	1
1.2 STEP-INDEX FIBRE	2
1.3 PHOTONIC CRYSTAL FIBRE.....	3
1.3.1 Solid-core photonic crystal fibre.....	3
1.3.2 Hollow-core photonic crystal fibre	4
1.3.3 Porous-core photonic crystal fibre	5
1.4 PHOTONIC CRYSTAL FIBRE AND TERAHERTZ WAVE TRANSMISSION	5
CHAPTER 2 Simulation: Finite Element Method	6
2.1 COMSOL MULTIPHYSICS SOFTWARE	6
2.2 FINITE ELEMENT METHOD	7
2.3 PERFECTLY MATCHED LAYER.....	7
CHAPTER 3 Optical Properties: Formulation	8
3.1 CONFINEMENT LOSS	8
3.2 EFFECTIVE MATERIAL LOSS.....	8
3.3 EFFECTIVE MODE AREA	9
3.4 NONLINEARITY COEFFICIENT	9
3.5 NUMERICAL APERTURE.....	9
3.6 POWER FRACTION.....	9
3.7 V-PARAMETER.....	10
CHAPTER 4 Heptagonal Photonic Crystal Fibre	11
4.1 PROPOSED HC PCF DESIGN	11
4.2 SIMULATION ANALYSIS	12
4.2.1 Varying frequency	12
4.2.2 Varying AFF	13

CHAPTER 5 Octagonal Photonic Crystal Fibre	15
5.1 PROPOSED SC O-PCF DESIGN	15
5.2 SIMULATION ANALYSIS	16
CHAPTER 6 Spider-Web Photonic Crystal Fibre	20
6.1 PROPOSED SW PCF DESIGN.....	20
6.2 SIMULATION ANALYSIS	21
CHAPTER 7 Results and Comparison	25
Conclusion	26
Future Work	27
References	28
List of Publications	31
APPENDIX 1: Thesis Plagiarism Report	32
APPENDIX 2: Manuscript of Paper - 1	37
APPENDIX 3: Manuscript of Paper - 2	43
APPENDIX 4: Manuscript of Paper - 3	48

List of Figures

1.1 (a) step-index fibre in multimode; (b) step-index fibre in mono-mode	2
1.2 Hexagonal arrangement of PCF	4
1.3 Hollow-core PCF	4
1.4 PCF having a porous core	5
2.1 COMSOL Multiphysics	6
2.2 (a) wave-equation problem from which some wave scattered into infinite space, (b) a perfectly matched layer is absorbing the wave	7
4.1 Proposed HC PCF	11
4.2 Fundamental mode at 1 THz for (a) x-polarization, and (b) y-polarization	12
4.3 Variation of confinement loss with frequency	13
4.4 Variation of EML with frequency	13
4.5 Variation of effective mode area with frequency	14
4.6 Variation of γ with frequency	14
4.7 Variation of confinement loss with a diameter of air holes	14
5.1 Initial arrangement to make SC O-PCF	15
5.2 Proposed SC O-PCF	16
5.3 Fundamental mode at 1 THz for (a) x-polarization, and (b) y-polarization	17
5.4 Variation of confinement loss with frequency (fused silica and Teflon)	17
5.5 (a) Variation of EML with frequency (fused silica)	18
5.5 (b) Variation of EML with frequency (Teflon)	18
5.6 Variation of effective mode area with frequency (fused silica and Teflon)	18
5.7 Variation of γ with frequency (fused silica and Teflon)	19
6.1 Cross-sectional view of the SW PCF with the fundamental mode at 1 THz	20
6.2 Confinement loss as a function of frequency	21
6.3 Effective material loss as a function of frequency	21
6.4 Effective mode area as a function of frequency	22
6.5 Nonlinearity coefficient as a function of frequency	22
6.6 Numerical aperture as a function of frequency	23
6.7 Power fraction as a function of frequency	23
6.8 V-parameter as a function of frequency	24

List of Tables

Table 7.1 Comparison of recent articles with proposed designs.....	25
--	----

List of Abbreviations/Symbols

ϵ	Dielectric permittivity of the medium.
μ	Magnetic permeability of the medium.
PCF	Photonic crystal fibre.
TIR	Total internal reflection.
AFF	Air-filling fraction.
FEM	Finite element method.
PML	Perfectly matched layer.
EML	Effective material loss.
NA	Numerical aperture.
ϵ_0	Dielectric permittivity of air/vacuum.
μ_0	Magnetic permeability of air/vacuum.
HC	Heptagonal cladding.
SC	Solid core.
SW	Spider-web.

Chapter 1

Introduction

Photonic crystals that work on the periodic arrangement of dielectric materials have three major types – (i) one-dimensional, (ii) two-dimensional, and (iii) three-dimensional, which are arranged periodically according to their dimensions. When Yablonovitch and John [1] published two milestones on photonic crystals, massive progress in this field was reported. Numerous applications of photonic crystals have existed since 1987, such as low-loss optical waveguides, Bragg reflectors, photonic crystal fibre (PCF), and so on. Photonic crystal fibres differ from conventional fibres and work on photonic band gaps and sometimes total internal reflections [2]. To understand the photonic crystal fibres, let us begin with step-index fibres.

1.1 ELECTROMAGNETIC WAVES

The propagation of light in an optical fibre is considered based on Maxwell's equations [3]. In a medium, when conductivity is zero, these equations can be written as

$$\nabla \times \mathbf{E} = -\frac{\partial \mathbf{B}}{\partial t} \quad (1.1)$$

$$\nabla \times \mathbf{H} = \frac{\partial \mathbf{D}}{\partial t} \quad (1.2)$$

where ∇ is a vector operator, $\mathbf{D} = \epsilon \mathbf{E}$, and $\mathbf{B} = \mu \mathbf{H}$. The divergence conditions in the absence of free charges and free poles are $\nabla \cdot \mathbf{D} = \mathbf{0}$ and $\nabla \cdot \mathbf{B} = \mathbf{0}$, respectively. Substituting \mathbf{D} and \mathbf{B} while taking the curl of equations (1.1) and (1.2) gives:

$$\nabla \times (\nabla \times \mathbf{E}) = -\mu \epsilon \frac{\partial^2 \mathbf{E}}{\partial t^2} \quad (1.3)$$

$$\nabla \times (\nabla \times \mathbf{H}) = -\mu \epsilon \frac{\partial^2 \mathbf{H}}{\partial t^2} \quad (1.4)$$

Then using the divergence conditions on equations (1.3) and (1.4) with the vector identity $\nabla \times (\nabla \times \mathbf{A}) = \nabla(\nabla \cdot \mathbf{A}) - \nabla^2 \mathbf{A}$, we obtain:

$$\nabla^2 \mathbf{E} = \mu\epsilon \frac{\partial^2 \mathbf{E}}{\partial t^2} \quad (1.5)$$

$$\nabla^2 \mathbf{H} = \mu\epsilon \frac{\partial^2 \mathbf{H}}{\partial t^2} \quad (1.6)$$

where ∇^2 is the Laplacian operator. The above equation satisfies every field vector component in the rectangular cartesian coordinate and cylindrical polar coordinates. The general solution of this equation is a sinusoidal wave. Which comes out to be:

$$\psi = \psi_0 \exp[j(\omega t - \mathbf{k} \cdot \mathbf{r})] \quad (1.7)$$

where \mathbf{k} is the propagation vector, $k = 2\pi/\lambda$.

1.2 STEP-INDEX FIBRE

A step-index or conventional fibre is an arrangement of core-cladding structures that works on total internal reflection. When the light falls between the boundary of two surfaces having different refractive indices, a part of it gets reflected. In contrast, another part gets refracted into the medium once the incidence angle exceeds the critical angle. In conventional fibre, refractive index (n_1) of the core of the fibre is higher than the refractive index (n_2) of the cladding.

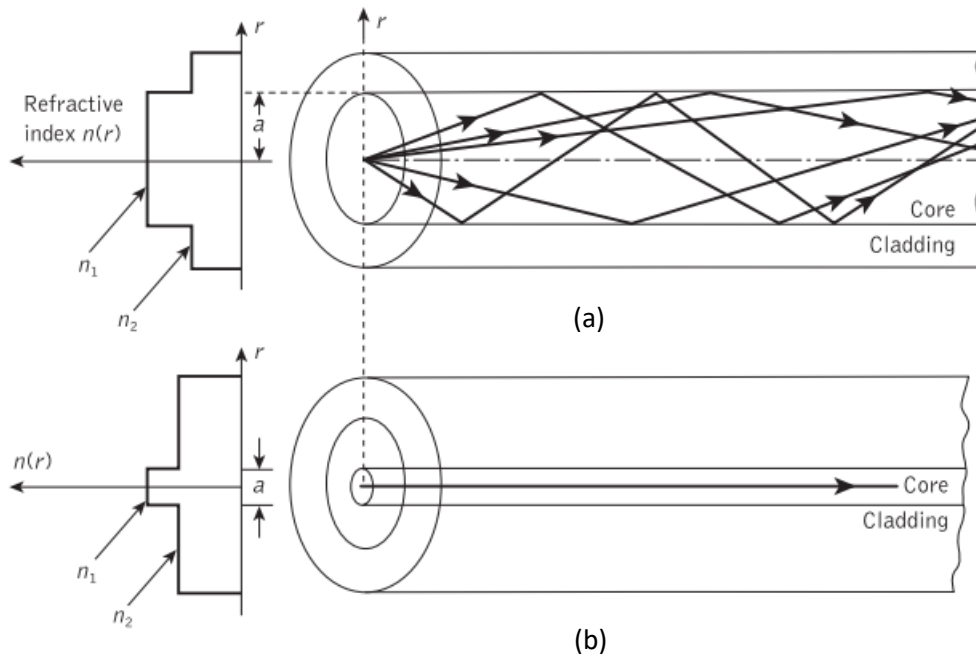


Fig. 1.1. (a) step-index fibre in multimode; (b) step-index fibre in mono-mode Ref. [3].

Figure 1.1(a) has a core radius of about $25 \mu m$ that allows the propagation of different modes within the core, which makes it a multimode step index fibre. Figure 1.1(b) depicts only the fundamental mode fibre, which allows the propagation of a single transverse electromagnetic wave. The order of its radius varies between 1 to $5 \mu m$.

1.3 PHOTONIC CRYSTAL FIBRE

In 1995, a new type of fibre, named photonic crystal fibre (PCF) [4], came into existence. These periodic fibres have low-index material and high-index material. Generally, PCFs' background or core material is silica and air holes in the cladding region typically provide the low-index material. There are numerous applications of PCFs have been reported; (i) non-telecom applications such as supercontinuum generation, (ii) high-speed transmission such as terahertz wave transmission, and so on [5]. There are three types of PCFs:

- a. Solid-core PCF,
- b. Hollow-core PCF, and
- c. Porous-core PCF.

1.3.1 Solid-core photonic crystal fibre

A fundamental or mono-mode PCF arrangement, in which the core is filled with high refractive index material and the cladding region is filled with multiple air holes, is known as solid-core PCF. Due to the high birefringence, large mode area, and flat dispersion curve with fundamental modes, these fibres open new opportunities in broadband transmission, sensors, etc. These fibres work on the principle of total internal reflection because the solid core behaves as a high-refracting medium. The wave is propagated to the lower refractive index, resulting in multiple reflections inside the core.

Figure 1.2 shows a type of solid core PCF[6]; here, the cladding region is filled with a hexagonal arrangement of air holes that have a specific air filling fraction (AFF) (it is the ratio of the diameter of air holes to the distance between two consecutive air holes, also known as pitch). The centralised air hole is removed to form the typical arrangement of the PCF. As mentioned above, this PCF has silica as the core or back material, whereas air holes are distributed in the cladding region.

$$AFF = \frac{\text{Diameter } (d)}{\text{Pitch } (\Lambda)} \quad (1.8)$$

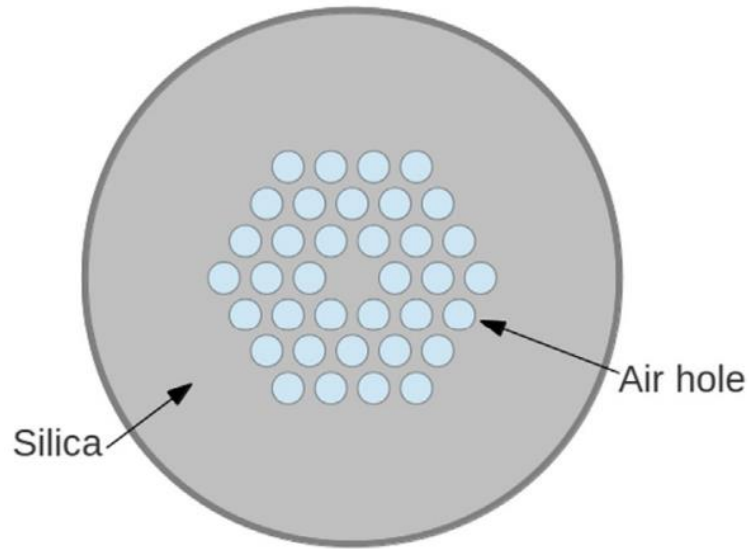


Fig. 1.2. Hexagonal arrangement of PCF Ref. [6].

1.3.2 Hollow-core photonic crystal fibre

A hollow-core photonic crystal fibre is a unique way of wave transmission of light in the air through the core [7]. Various capillaries surround the hollow core in different manners into the cladding region, shown in Fig. 1.3 [8]. Such a PCF works on the principle of photonic band gap (PBG) that states: 'preventing of light of certain frequencies or wavelengths from different polarisation directions such as one – dimensional, two – dimensional, and three – dimensional'. These fibres have the main advantage of minimising loss due to the dielectric and can be used in gas-laser transmission, pulse compression, etc.

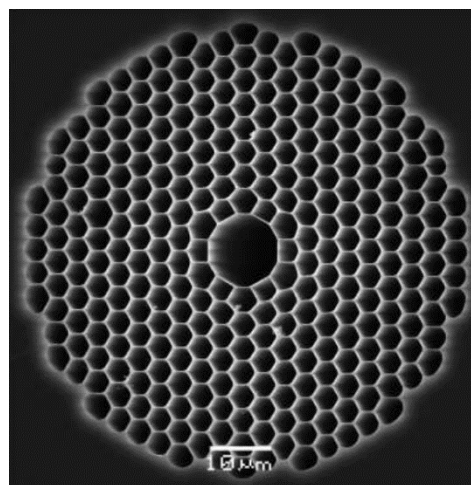


Fig. 1.3. Hollow-core PCF Ref. [8].

1.3.3 Porous-core photonic crystal fibre

A porous-core arrangement can be said as a mixture of solid-core and hollow-core in which air holes are discontinuously arranged in the solid material of the core. Air holes in the cladding region can be etched similarly to the other two PCFs. Inside the core, various designs, such as circular shapes, elliptical shapes, air holes, etc., have been fused [9]. Due to the low index in the core, it reduces the frequency-dependent refractive index of the PCF. Figure 1.4 [10] shows the circular core hole arrangement of the porous core PCF.

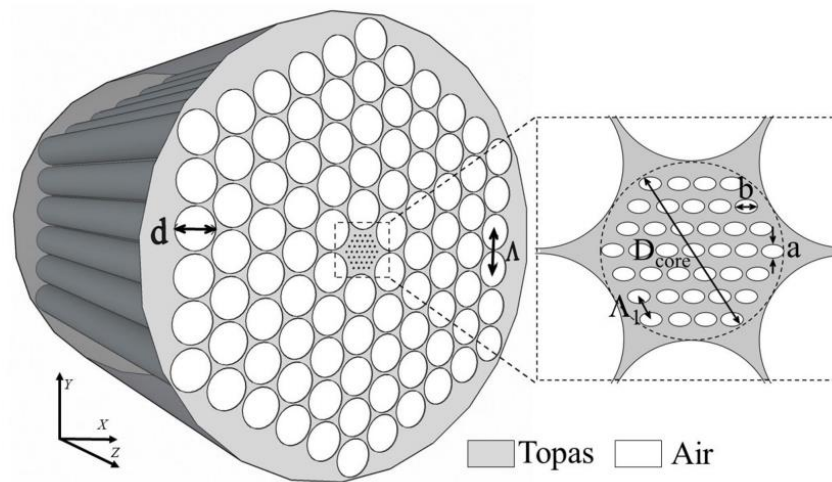


Fig. 1.4. PCF having a porous core Ref. [10].

1.4 PHOTONIC CRYSTAL FIBRE AND TERAHERTZ WAVE TRANSMISSION

On the electromagnetic spectrum, terahertz radiation lies between infrared and microwave region with frequency ranging from 0.1 to 10 THz. Terahertz radiation is also known as submillimetre radiation, have numerous applications such as surveillance, imaging, communications, spectroscopy, and so on [11]. Constructing PCF for terahertz waveguide is challenging due to their longer wavelength; however, materials like silica, Teflon, Topas, Zeonex, poly-methyl methacrylate (PMMA), chalcogenide glass, etc., can be introduced in the core for guiding mechanism. The materials mentioned above are preferred to capture most radiation and minimise losses inside a fibre.

Simulation: Finite Element Method

In the emerging world of computing and simulation, sometimes it is challenging to fabricate an actual design or structure to know its reliability. The idea of simulating real-world designs has been advancing the human era. Multiphysics software like COMSOL Multiphysics Simulation, Ansys Multiphysics, RP Fibre, etc., can now build fundamental to advanced ideas of fibre or other physical designs, including their numerical calculations. These calculations can be achieved without fabricating in the laboratory.

2.1 COMSOL MULTIPHYSICS SOFTWARE

1986 Stockholm, Sweden, gave two geniuses to the emerging world of computation, Svante Littmarck and Farhad Saeidi, who launched COMSOL as simulation software and later named it COMSOL Multiphysics Software. COMSOL offers various physics modules such as AC/DC, electrochemistry, ray optics, wave optics, etc. Figure 2.1 shows the typical COMSOL software image used in this research [12].



Fig. 2.1. COMSOL Multiphysics Ref. [12].

2.2 FINITE ELEMENT METHOD

The finite element method (FEM) is a numerical method from computational electromagnetics that provides numerical simulations like the finite difference method; however, this method is a general and powerful approach to real-world applications. This method may include multi-physics simulation, complicated geometry, and boundary conditions applied while meshing in COMSOL. In FEM, the main domain is treated as a bunch of co-domains. On each co-domain, the governing equation, for example, electromagnetic wave equations, is applied by any suitable numerical method. This method works on the principle of piece-wise approximation of a function because it is easy to define them as simple polynomials [13].

4.1 PERFECTLY MATCHED LAYER

A perfectly matched layer or PML is a boundary condition used to truncate any numerical errors from the structure. For example, it is essential to truncate the computational errors while solving partial differential equations numerically by volume discretisation. The artefact is applied so that it does not disturb the geometry. In numerical optics, two main components, (i) confinement loss and (ii) effective material loss (EML), is calculated using the perfectly matched layer. It holds the property of wave transmission into the infinite space from the core to the fibre cladding. The PML measures the coming wave from the core. Figure 2.2 depicts a similar situation [14].

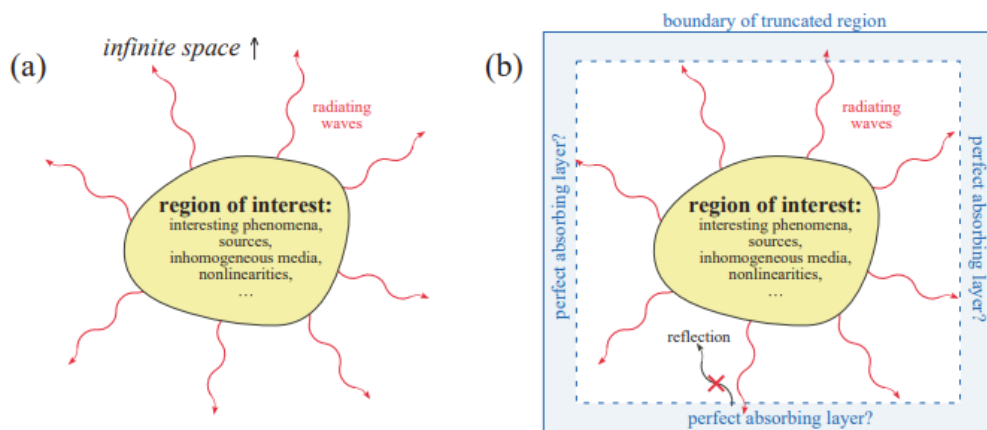


Fig. 2.2. (a) Wave-equation problem from which some wave scattered into infinite space, (b) a perfectly matched layer is absorbing the wave Ref. [14].

Optical Properties: Formulation

Various optical properties can be observed in PCF from varying frequencies or wavelengths to produce variation in air holes, i.e., AFF. The optical properties include effective mode index, effective material loss (EML), confinement loss, etc. These properties of the fibre conclude the reliability of fibre [15]. In the last decade, research on PCFs has shown that various losses have been minimised, and essential event such as effective mode area has been improved that emerge the use of PCFs in the application of broadband transmission, sensors, and filters. In the below sections, seven different optical parameters have been discussed.

3.1 CONFINEMENT LOSS

The confinement loss depicts the radiation confinement in the core. Whenever the radiation gets leaked from the fibre, a numerical truncation layer, i.e., PML, is used to measure the proportion of radiation. The confinement loss can be calculated using the imaginary part of the effective mode index for the fundamental mode. The relation is as follows [16]:

$$L \left[\frac{dB}{cm} \right] = 8.686k_0 \text{Im}(n_{eff}) \times 10^{-2} \quad (3.1)$$

where $\text{Im}(n_{eff})$ is the imaginary part of the effective mode index for the fundamental mode and $k_0 = \frac{2\pi\nu}{c}$.

3.2 EFFECTIVE MATERIAL LOSS

Like confinement loss, effective material loss (EML or α_{eff}) is calculated from the perfectly matched layer (PML). The ratio of the integral over the dielectric of the fibre to the integral over the whole of the fibre shows the amount of radiation absorbed by the fibre. This can be evaluated using the following relation [17]:

$$\alpha_{eff} \left[\frac{dB}{cm} \right] = \sqrt{\frac{\epsilon_0}{u_0}} \frac{\int_{mat} n_{mat} \alpha_{mat} |E|^2 dA}{2 \left| \int_{all} S_z dA \right|} \quad (3.2)$$

where s_z is the pointing vector, n_{mat} is the refractive index of the material, and α_{mat} is bulk material absorption loss.

3.3 EFFECTIVE MODE AREA

The area acquired by the fundamental mode inside the core is another essential optical parameter that depicts the wave propagation confinement area. This can be observed using the following relation [18]:

$$A_{eff} [m^2] = \frac{\left[\int I(r) dr \right]^2}{\left[\int I^2(r) dr \right]} \quad (3.3)$$

3.4 NONLINEARITY COEFFICIENT

The nonlinearity coefficient (γ) can be improved by reducing the effective mode area. The A_{eff} decreases with an increase in the terahertz frequency; hence, the nonlinearity coefficient increases. The nonlinearity coefficient can be calculated as [19]:

$$\gamma = \frac{2\pi n_2}{\lambda A_{eff}} = \frac{2\pi v n_2}{c A_{eff}} \quad (3.4)$$

where n_2 is nonlinear refractive index of the material.

3.5 NUMERICAL APERTURE

The core's acceptance or emission of radiation is observed by calculating the numerical aperture (NA). It can be estimated as [20]:

$$NA = \frac{1}{\sqrt{1 + \frac{\pi A_{eff} v^2}{c^2}}} \quad (3.5)$$

3.6 POWER FRACTION

The power held by the fibre can be evaluated using [21]:

$$P = \frac{\int_i S_z dA}{\int_{All} S_z dA'} \times 100 \% \quad (3.6)$$

where s_z is the Poynting's vector integrated over material and the whole fibre.

3.7 V-PARAMETER

The V-parameter can be estimated using [22]:

$$V = \frac{2\pi r v}{c} \sqrt{n_{co}^2 - n_{cl}^2} \quad (3.7)$$

where n_{co} is the effective refractive index of the core, n_{cl} is the effective refractive index of the cladding, and r is the radius of the core.

Heptagonal Cladding Photonic Crystal Fibre

The chapter will discuss photonic crystal fibre with a heptagonal air-hole arrangement in the cladding region and core following the same pattern. The proposed design is simulated for four crucial optical parameters, i.e., confinement loss, EML, effective mode area, and nonlinearity coefficient. We have found very few research articles on heptagonal cladding (HC) that may have two reasons, (i) the mathematical modelling is complex, (ii) due to gaps in successive rings, losses cannot be minimised ideally.

4.1 PROPOSED HC PCF DESIGN

The heptagonal cladding (HC) PCF can be made by selecting one circular air hole distanced from the centre depending on the diameter of the core (d_{core}). From the

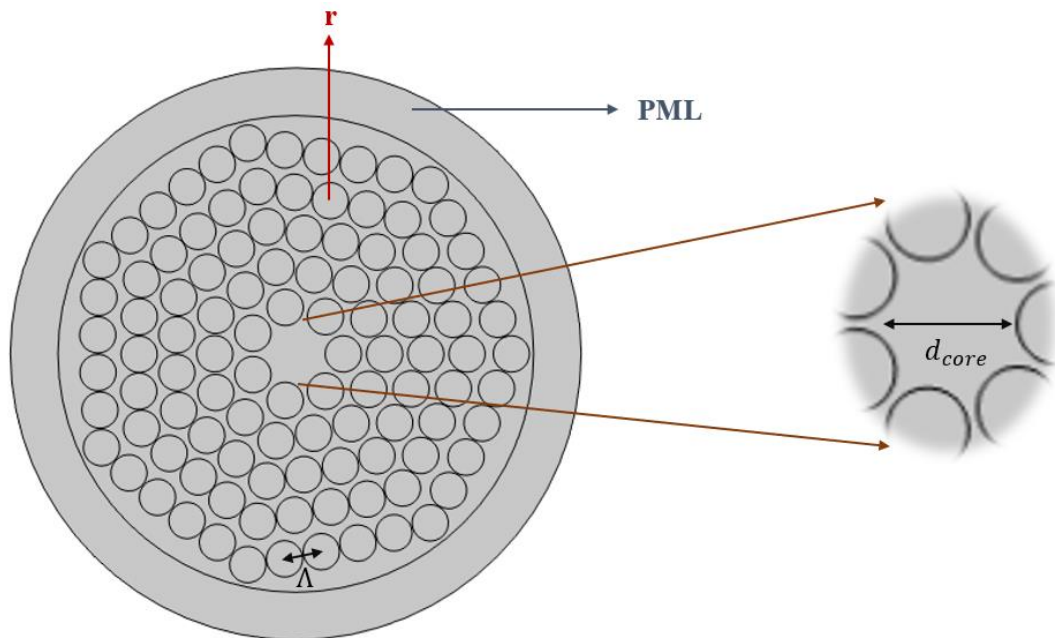


Fig. 4.1. Proposed HC PCF.

geometrical transformation of the COMSOL, by using ‘copy’, revolve multiple air holes at $\theta = \frac{2\pi n}{7}$, where $n = 1, 2, 3, 4, 5,$ and 6 . Repeat the same steps for multiple heptagonal

air-hole rings but place the first air-hole at some other point which should be more than the previous case. Once all the air holes are arranged, a cladding and numerical layer must be installed, i.e., PML, 10 to 20% of cladding. We have used chalcogenide glass as a core material in this design to check the absorption of microwave radiation inside the fibre. PML must use the same material as the core because it is just a numerical boundary. Figure 4.1 depicts the proposed design of HC PCF. The core of it is decided to be a solid core only. For this design, cladding is taken to be 7.5 mm , $d_{core} = 3\text{ mm}$, and $\Lambda = 0.6$.

4.2 SIMULATION ANALYSIS

The proposed structure is simulated in two ways:

- i. by varying the terahertz frequency from 0.3 to 4.0 THz , all four parameters have been evaluated.
- ii. by varying AFF from 0.4 to 0.6 at 1 THz , confinement loss has been observed.

The x- and y- polarisation of light confinement in the core is depicted in Fig. 4.2. At 1 THz , the effective mode index is 2.60 . All graphs are plotted using the MATLAB algorithm.

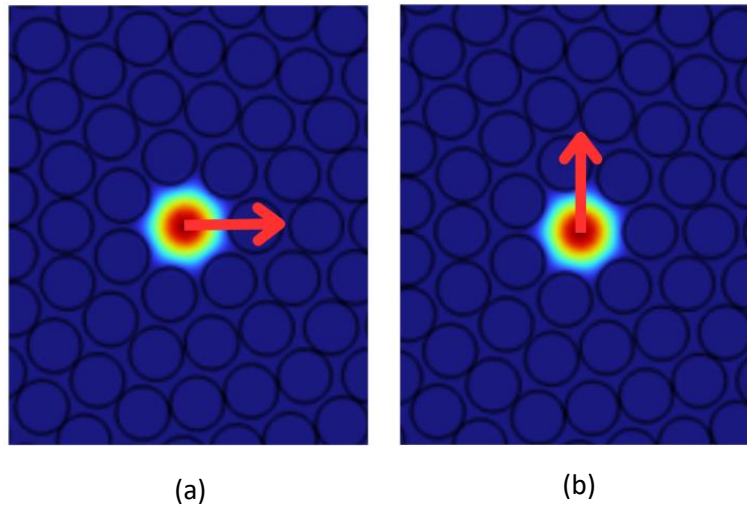


Fig. 4.2. Fundamental Mode at 1 THz for (a) x-polarization, and (b) y-polarization.

4.2.1 Varying frequency

- i. **Confinement loss:** With the varying frequency, confinement loss for this design is reported as low as $3.91 \times 10^{-15}\text{ dB/cm}$, which increases with the increase in frequency and said maximum value at 4.0 THz of $4.06 \times$

$10^{-13} dB/cm$. Figure 4.3 shows the variation of confinement loss with terahertz frequency.

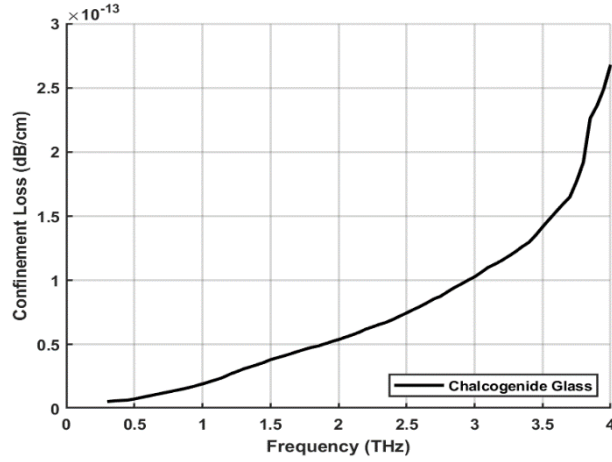


Fig. 4.3. Variation of confinement loss with frequency.

ii. **Effective material loss:** Due to using chalcogenide glass, at 0.3 THz, EML is reported $1.28 \times 10^{-2} dB/cm$ only. Figure 4.4 shows the variation of it.

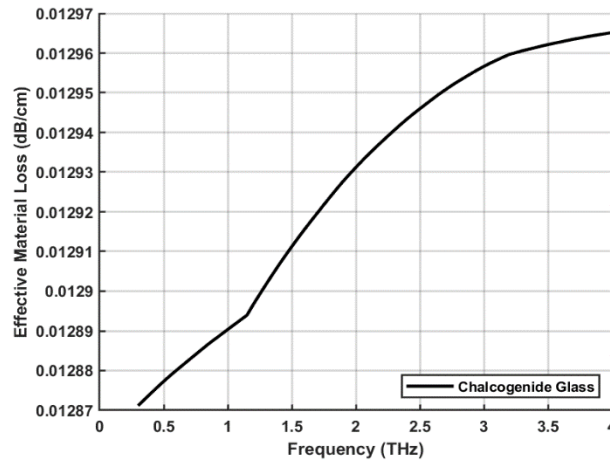


Fig. 4.4. Variation of EML with frequency.

iii. **Effective mode area:** Figure 4.5 shows the variation of the fundamental mode area, which has the highest value of $2.04 \times 10^{-6} m^2$ and decreases to the lowest value with increasing frequency.

iv. **Nonlinearity coefficient:** The nonlinearity coefficient varies inversely with the effective mode area. Figure 4.6 shows the variation and compares it with the effective mode area. Both graphs run conversely.

4.2.2 Varying AFF

The confinement loss has decreased with an increase in AFF because high AFF blocks the light entering the PML. Figure 4.7 depicts the variation of confinement loss with AFF.

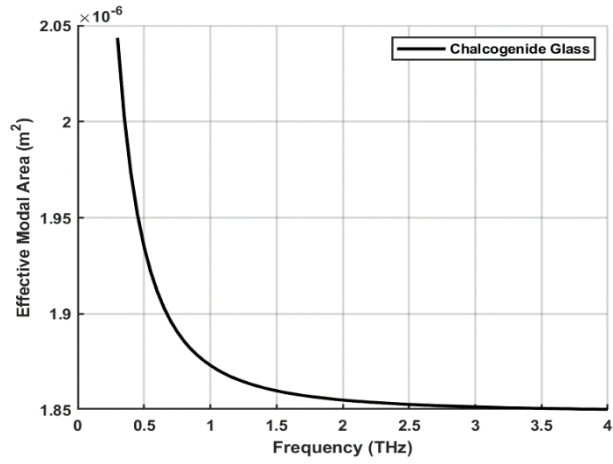


Fig. 4.5. Variation of effective mode area with frequency.

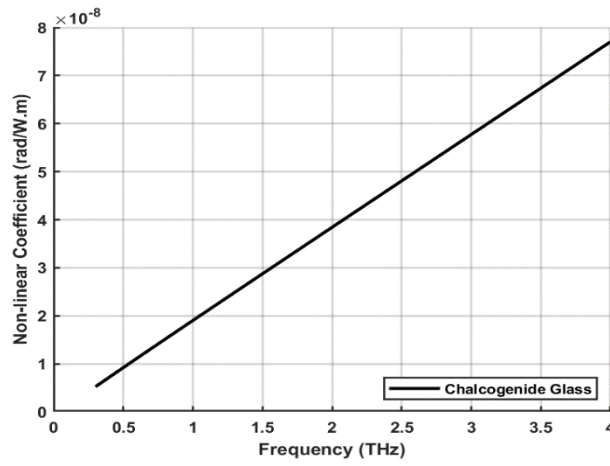


Fig. 4.6. Variation of γ with frequency.

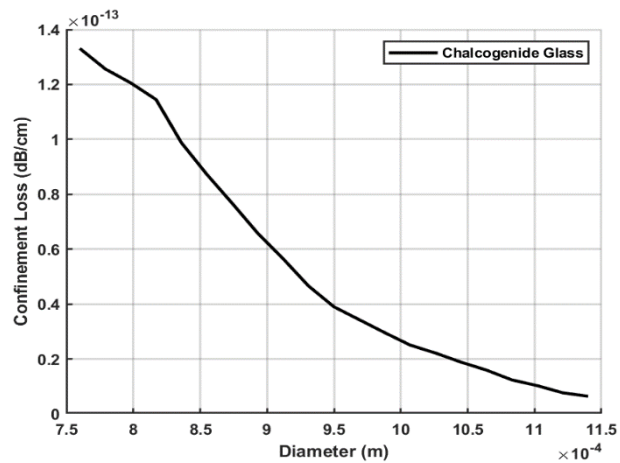


Fig. 4.7. Variation of confinement loss with diameter of air holes.

Octagonal Cladding Photonic Crystal Fibre

The chapter will discuss photonic crystal fibre with an octagonal air-hole arrangement in the cladding region and core following the same pattern. The proposed design is simulated for four crucial optical parameters, i.e., confinement loss, EML, effective mode area, and nonlinearity coefficient. The core of this design is solid; hence, named solid core (SC) octagonal PCF (O-PCF). From this design, we could minimise losses and maximise the effective mode area.

5.1 PROPOSED SC O-PCF DESIGN

The proposed octagonal cladding PCF can be made by the following algorithm in COMSOL geometry:

- i. choose a centralised circle at $(0, 0)$ coordinates.
- ii. select ‘Array’ from the transformation window and select the first circle to create two more circles adjacent to it.

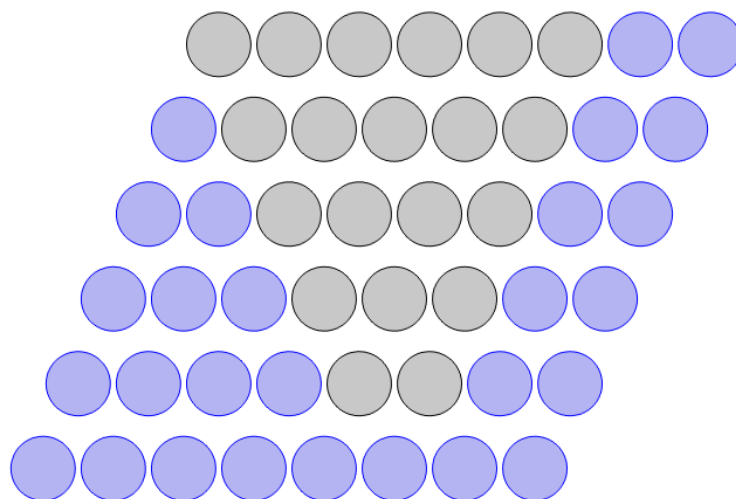


Fig. 5.1. Initial arrangement to make SC O-PCF.

- iii. select the ‘Array’ command again and make more linear circles towards the right that make seven circles.
- iv. the following ‘Array’ command will transform the linear seven air holes line in xy-plane as shown in Fig. 5.1.
- v. using the ‘Delete entities’ command, delete the circles highlighted in Fig. 5.1.
- vi. unshaded shape triangle can be rotated using $\frac{2\pi n}{8}$, where $n = 1, 2, 3, 4, 5, 6, \text{ and } 7$. Once the cladding shape is formed, infused PML and cladding keeping the core solid.

Figure 5.2 shows the proposed O-PCF design. The core or back material of this PCF is fused silica and Teflon to make a comparison among them.

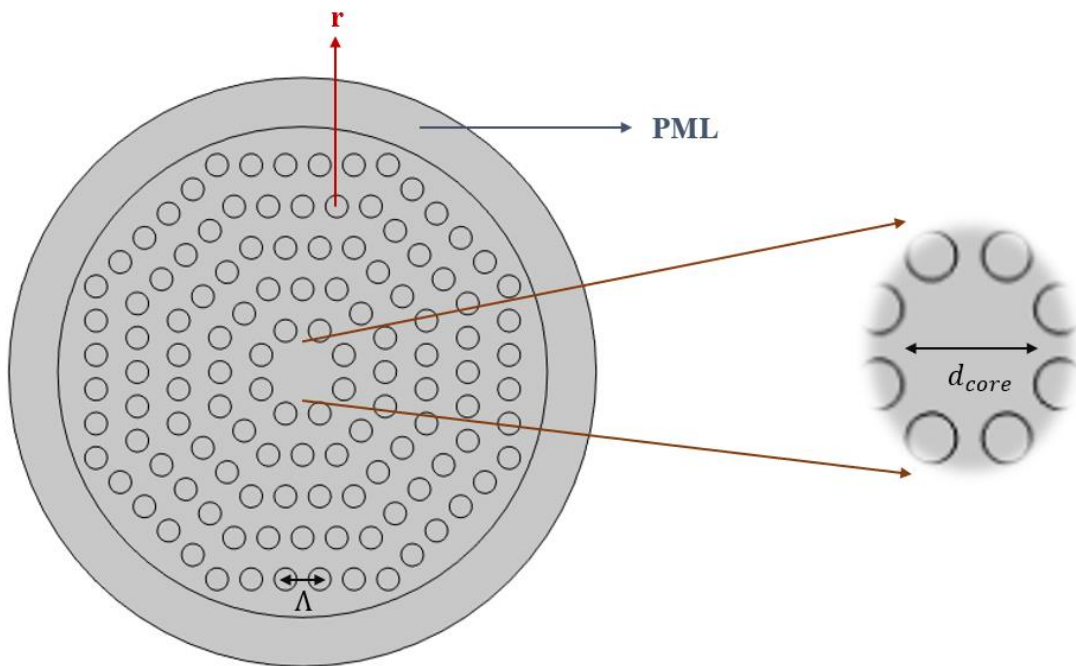


Fig. 5.2. Proposed SC O-PCF.

5.2 SIMULATION ANALYSIS

For the simulation of the proposed design, AFF is taken as a constant of value $\Lambda = 0.5$. The $d_{core} = 0.95mm$, the cladding is $10.4mm$, and infused precisely 20% of the cladding. In this design with the fused silica and Teflon, better results have been reported compared to heptagonal cladding PCF, as mentioned in Chapter – 4. The simulation is done with varying terahertz frequencies from 0.7 to 3.0 THz. Figure 5.3 represents the x- and y- polarisation of light inside the core.

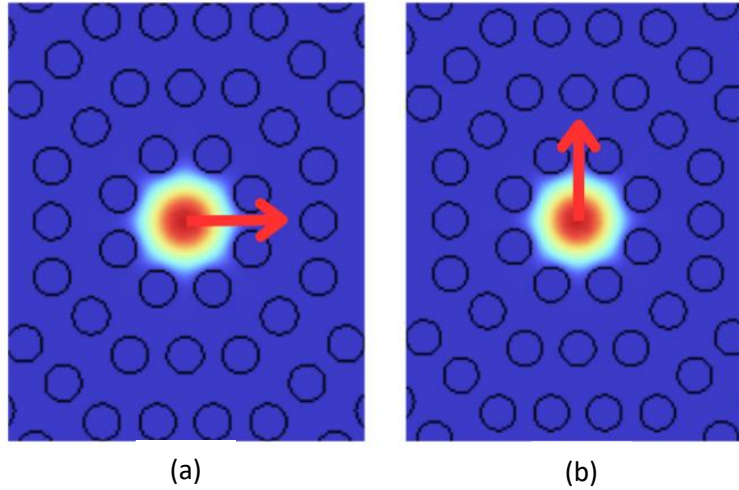


Fig. 5.3. Fundamental Mode at 1 THz for (a) x-polarization, and (b) y-polarization.

- i. Confinement loss:* Figure 5.4 provides the information regarding the comparison between the fused silica and Teflon materials' confinement loss which is as low as 10^{-15} dB/cm .

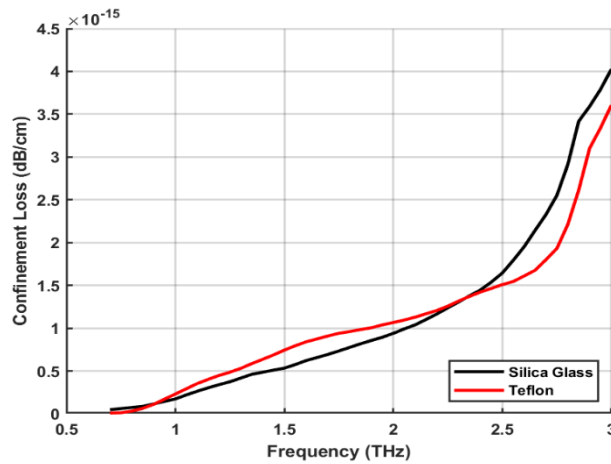


Fig. 5.4. Variation of confinement loss with frequency (fused silica and Teflon).

- ii. EML:* Figures 5.5 (a) and (b) show the EML of the fused silica and Teflon, respectively. It is noted that the value of EML is in the range of bulk material absorption loss for both materials; hence, this argument increases the reliability of the fibre.
- iii. Effective mode area:* Figure 5.6 illustrates the high effective mode area at a lower frequency for both materials, but these values decrease with increased terahertz frequency.

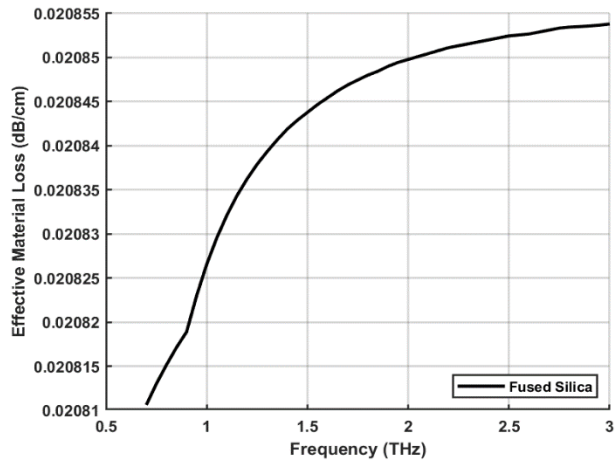


Fig. 5.5 (a). Variation of EML with frequency (fused silica).

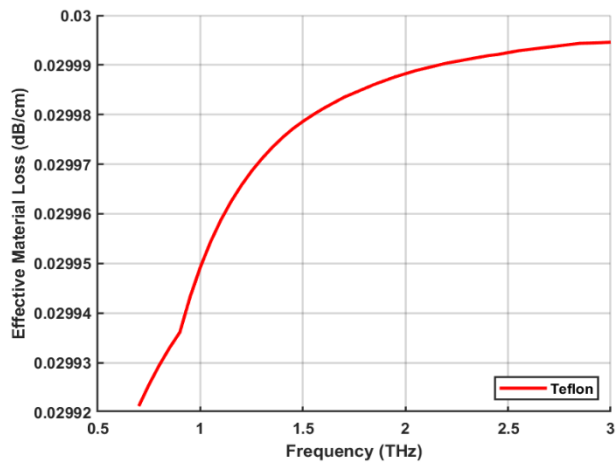


Fig. 5.5 (b). Variation of EML with frequency (Teflon).

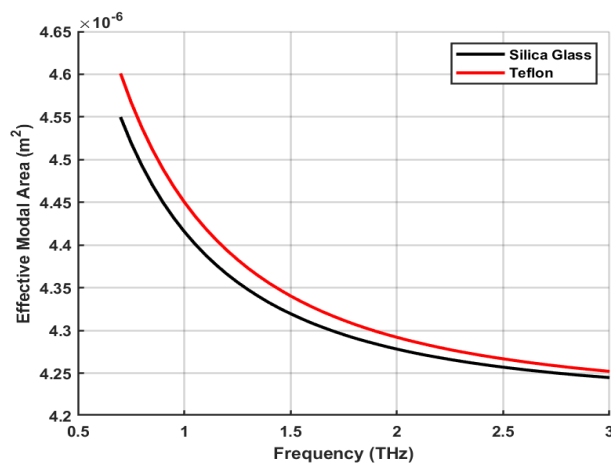


Fig. 5.6. Variation of effective mode area with frequency (fused silica and Teflon).

iv. Nonlinearity coefficient: The nonlinearity coefficient increases with decreasing in effective mode area; Fig. 5.7 portrays a similar situation.

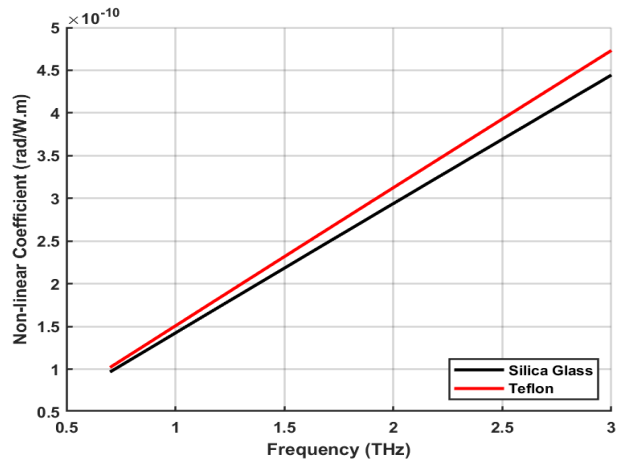


Fig. 5.7. Variation of γ with frequency (fused silica and Teflon).

Spider-Web Cladding Photonic Crystal Fibre

In this chapter, we have introduced a unique design. The PCF cladding is now beautifully designed with air holes like a Spider-Web (SW), and the core is approximated circularly. Seven optical parameters, named confinement loss, EML, effective mode area, nonlinearity coefficients, numerical aperture (NA), power fraction, and V-parameter, have been discussed to know the uniqueness of this PCF. The core of this design is solid and infused with fused silica.

6.1 PROPOSED SW PCF DESIGN

As discussed in Chapter – 5, this design can be made in a similar fashion by putting the first air hole at some distance away from the centre. In the core region, twenty air holes are punched to make the core circular. Figure 6.1 illustrates the SW PCF design. In

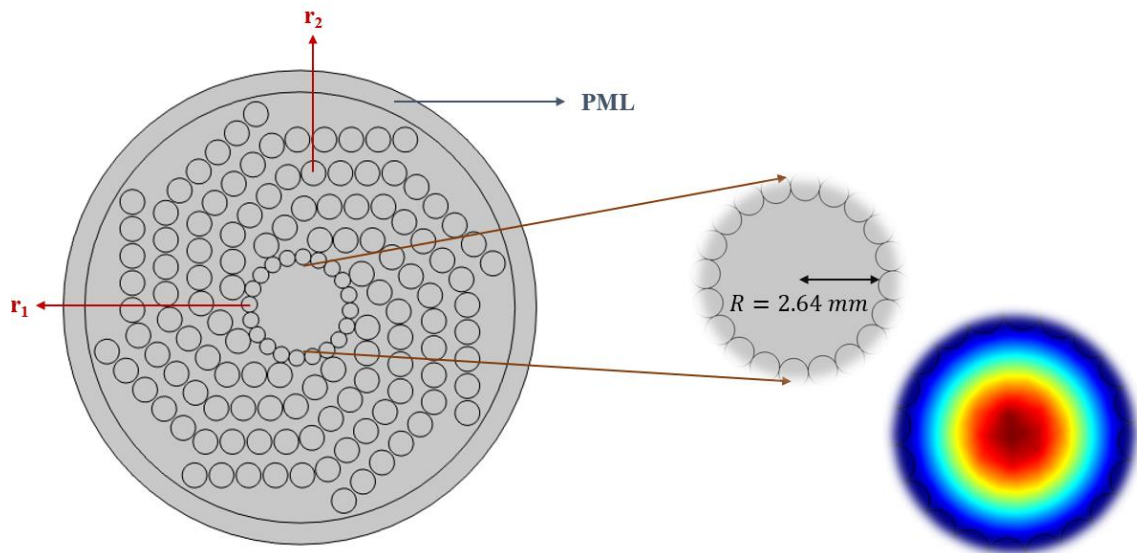


Fig. 6.1. Cross-sectional view of the SW PCF with the fundamental mode at 1 THz.

the cladding, $r_1 = 213 \mu\text{m}$ with AFF 0.45 and $r_2 = 332.5 \mu\text{m}$ with AFF 0.7. The PML is taken 10% of the cladding, and the core diameter is 5.28 mm. The core is infused with fused silica due to its constant bulk material absorption loss.

6.2 SIMULATION ANALYSIS

There may have multiple factors that have to be considered while simulating this fibre; however, we have chosen to vary it with frequency ranging from 0.1 to 3.0 THz. The optical properties of SW PCF are as follows:

- i. Confinement loss:* In this design, the lowest confinement loss has been reported at 0.1 THz, which is increased to the maximum value of just $8.35 \times 10^{-16} \text{ dB/cm}$. Figure 6.2 portrays the variation.

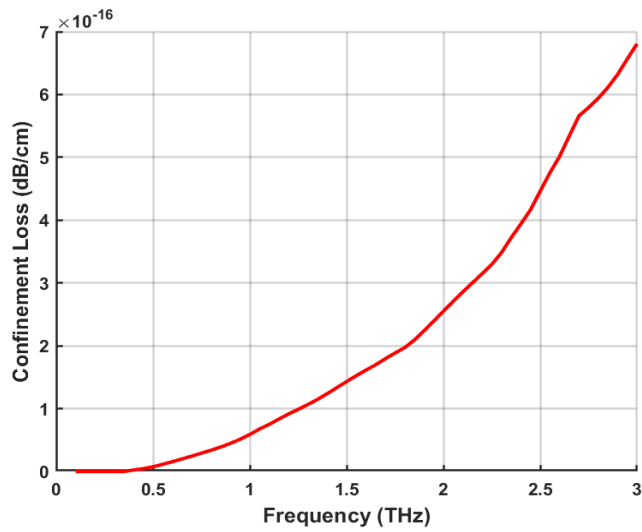


Fig. 6.2. Confinement loss as a function of frequency.

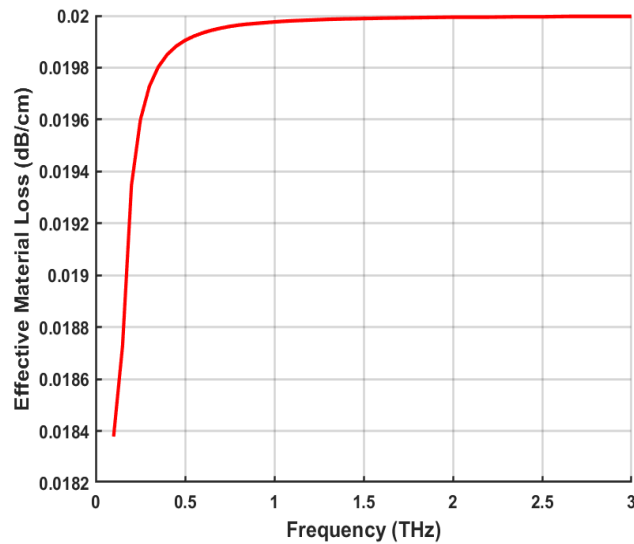


Fig. 6.3. Effective material loss as a function of frequency.

- ii. **EML:** Due to the constant bulk material absorption loss, the EML is as low as $1.99 \times 10^{-2} \text{ dB/cm}$, which reaches the value of bulk material. Figure 6.3 illustrates the increasing material loss with frequency.
- iii. **Effective mode area:** This design has reported the maximum effective mode area of $1.08 \times 10^{-5} \text{ m}^2$, portrayed in Fig. 6.4, demonstrating that this fibre is capable of high broadband transmission.

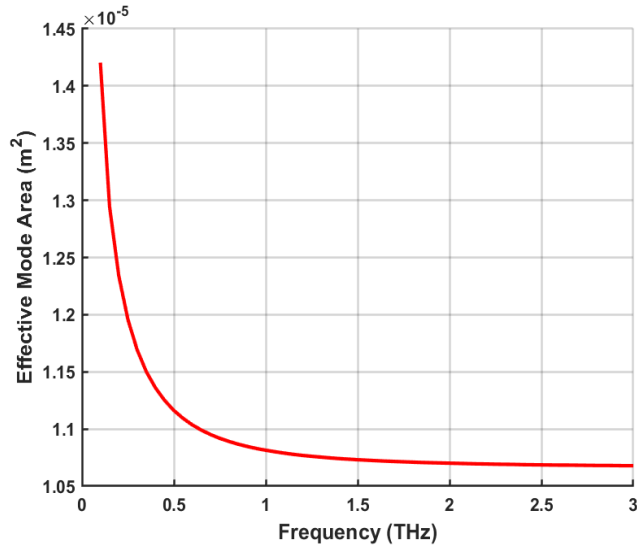


Fig. 6.4. Effective mode area as a function of frequency.

- iv. **Nonlinearity coefficient:** Nonlinearity varies inversely with the effective mode area. Figure 6.5 clarifies these variations.

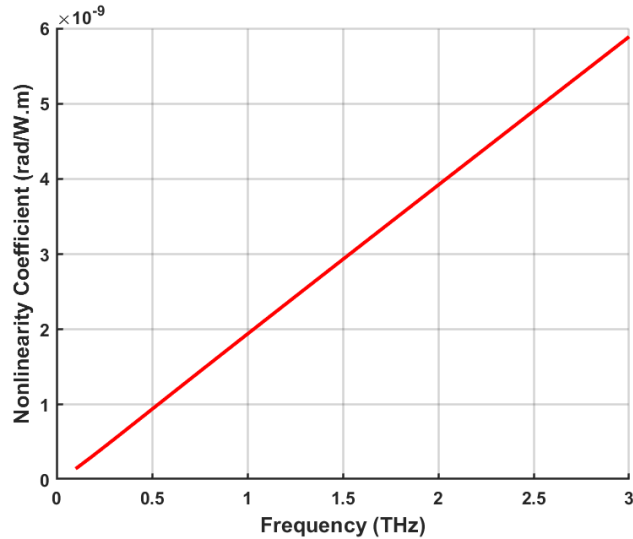


Fig. 6.5. Nonlinearity coefficient as a function of frequency.

- v. **Numerical aperture:** The numerical aperture can understand the core's acceptance or emission of radiation strength. The highest value of radiation

strength is reported 0.41 at 0.1 THz. Figure 6.6 shows the variation of numerical aperture with frequency.

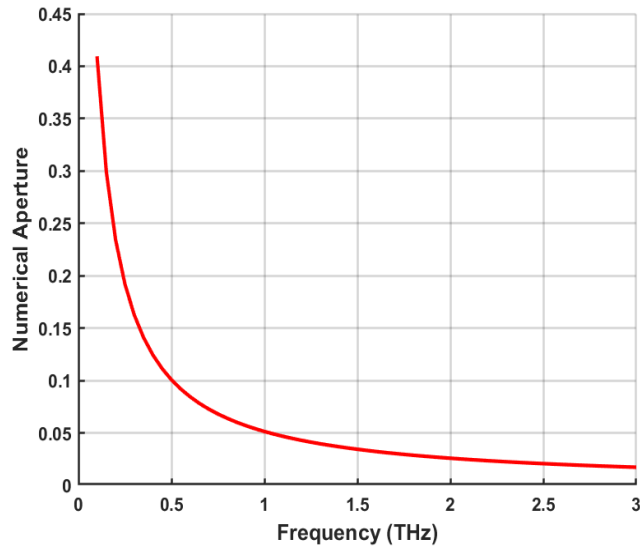


Fig. 6.6. Numerical aperture as a function of frequency.

- vi. Power fraction:* In the mono-mode fibres, the more power is confined to the core qualifies the fibre for its huge applications range. Figure 6.7 provides information on power with varying frequencies.

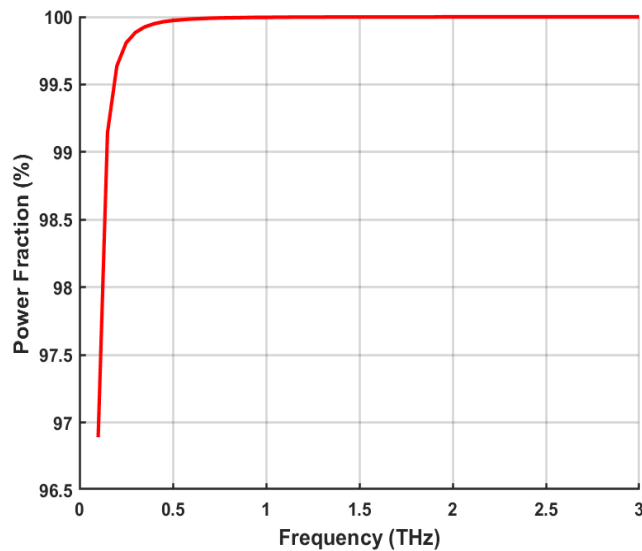


Fig. 6.7. Power fraction as a function of frequency.

- vii. V-parameter:* Characteristic property of fibre is concluded with V-parameter. It should be varied linearly with frequency to make fibre a success. Figure 6.8 shows a similar variation.

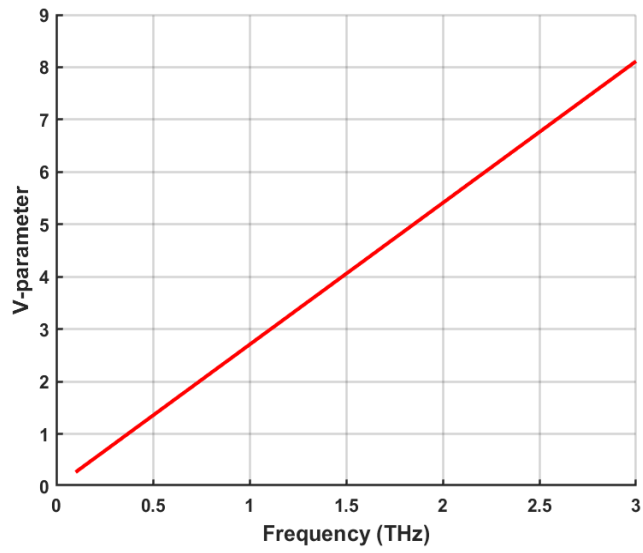


Fig. 6.8. V-parameter as a function of frequency.

Chapter 7

Results Comparison

Table 7.1 shows the comparison between Ref. [23-30] with HC PCF (mentioned in Chapter – 4), SC O-PCF (mentioned in Chapter – 5), and SW PCF (mentioned in Chapter – 6).

Table 7.1. Comparison of Ref. [23-30] with proposed designs.

Ref.	$EML (cm^{-1})$	$L (cm^{-1})$	$A_{eff}(m^2)$	$\gamma(rad/W.m)$	NA	$Power \%$
[23]	6.0×10^{-2}	5.45×10^{-13}	1.20×10^{-7}	-	-	44
[24]	8.0×10^{-2}	3.20×10^{-13}	1.20×10^{-7}	-	-	57
[25]	5.0×10^{-2}	7.79×10^{-12}	2.0×10^{-5}	-	-	-
[26]	-	10^{-9}	5.62×10^{-6}	3.0×10^{-8}	-	-
[27]	6.60×10^{-2}	5.42×10^{-13}	1.10×10^{-7}	-	-	-
[28]	-	2.28×10^{-16}	1.49×10^{-7}	-	-	77
[29]	1.5×10^{-2}	3.80×10^{-13}	5.00×10^{-8}	-	0.50	-
[30]	5.0×10^{-2}	8.01×10^{-7}	1.50×10^{-6}	-	0.37	55
HC PCF	1.28×10^{-2}	3.91×10^{-15}	2.04×10^{-6}	5.23×10^{-9}	-	-
SC O-PCF (Fused Silica)	2.08×10^{-2}	1.66×10^{-16}	4.42×10^{-6}	1.42×10^{-10}	-	-
SC O-PCF (Teflon)	2.99×10^{-2}	2.83×10^{-16}	4.45×10^{-6}	1.51×10^{-10}	-	-
SW PCF	1.99×10^{-2}	6.22×10^{-17}	1.08×10^{-5}	2.03×10^{-9}	0.41	99

Conclusion

This thesis proposes three different designs, i.e., HC PCF, SC O-PCF, and SW PCF, in different materials with different refractive indices. All these designs are simulated within the range of 0.1 to 4.0 THz frequency. The lowest confinement loss is reported for SW PCF, which is $6.22 \times 10^{-17} \text{ dB/cm}$, and it gives the highest effective mode area of $1.08 \times 10^{-5} \text{ m}^2$, too. The seven optical properties have shown that these designs are more reliable and standalone in various PCF applications, such as high-broadband transmission, chemical sensors, biosensors, spectroscopy, telecommunication, and other terahertz applications in comparison to existing results. All proposed designs are mono-mode or fundamental mode fibres that allow radiation to transmit in one way. SC O-PCF can be a suitable choice among the proposed designs after SW PCF.

Future Work

In the emerging era of technology, human needs have been skyrocketing since the 1900s. In 1987, when two-dimensional photonic crystals came into the limelight of researchers, no one would have imagined how impactful they would be. The terahertz frequency is just a tiny proportion of the colossal application world of PCFs. In the future, we look forward to working on different PCF applications with the same design, such as supercontinuum generation. Moreover, there are other ideas to design PCFs' cladding with which the losses can be minimised to the following extent. In the future, working on porous core and hollow core fibres may open different views on PCFs for us and allow us to explore outside the mono-mode or fundamental mode fibres.

References

- [1] J. D. Joannopoulos, P. R. Villeneuve, and S. Fan, "Photonic crystals: putting a new twist on light," *Nature*, vol. 386, pp. 143–149, 1997.
- [2] J. C. Knight, "Photonic crystal fibres," pp. 847–851, 2003.
- [3] J. M. Senior, "Optical Fiber Communications Principles and Practice Third Edition Optical Fiber Communications Optical Fiber Communications Principles and Practice Third Edition," 2009.
- [4] F. Poli, A. Cucinotta, and S. Selleri, "Photonic Crystal Fibers: Properties and Applications," vol. 102. Springer Science & Business Media, 2007.
- [5] A. Bjarklev and C. Lin, "Applications of Photonic Crystal Fibers in Optical Communications---What is in the Future?," 2005.
- [6] Y. Bai and Q. Bai, "Subsea Pipeline Integrity and Risk Management." Gulf Professional Publishing, 2014.
- [7] F. Gérôme, R. Jamier, J.-L. Auguste, G. Humbert, and J.-M. Blondy, "Simplified hollow-core photonic crystal fiber," 2010.
- [8] A. Al Sheakh and A. A. prof Anwaar Al Dergazly, "Simulation of Hexagonal HC-PCF With Circular Holes using COMSOL Multiphysics Software," 2022.
- [9] I. K. Yakasai, P. E. Abas, and F. Begum, "Review of porous core photonic crystal fibers for terahertz waveguiding," *Optik (Stuttg)*, vol. 229, Mar. 2021, doi: 10.1016/j.ijleo.2021.166284.
- [10] E. Reyes-Vera, J. Usuga-Restrepo, C. Jimenez-Durango, J. Montoya-Cardona, and N. Gomez-Cardona, "Design of Low-loss and Highly Birefringent Porous-Core Photonic Crystal Fiber and Its Application to Terahertz Polarization Beam Splitter," *IEEE Photonics J*, vol. 10, no. 4, Aug. 2018, doi: 10.1109/JPHOT.2018.2860251.
- [11] M. Goto, A. Quema, H. Takahashi, S. Ono, and N. Sarukura, "Teflon Photonic Crystal Fiber as Terahertz Waveguide," *Japanese Journal of Applied Physics, Part 2: Letters*, vol. 43, no. 2 B, Feb. 2004, doi: 10.1143/jjap.43.1317.
- [12] "COMSOL Multiphysics Reference Manual," 1998. [Online]. Available: www.comsol.com/blogs
- [13] J. N. Reddy, "Introduction to the Finite Element Method," Fourth Edition. Mc Graw Hill Education, 2019.
- [14] S. G. Johnson, "Notes on Perfectly Matched Layers (PMLs)," 2008.

- [15] H. Li et al., “Prediction of the optical properties in photonic crystal fiber using support vector machine based on radial basis functions,” *Optik (Stuttg)*, vol. 275, Mar. 2023, doi: 10.1016/j.ijleo.2023.170603.
- [16] V. Finazzi, T. M. Monro, and D. J. Richardson, “Small-core silica holey fibers: nonlinearity and confinement loss trade-offs,” 2003.
- [17] M. M. Hasan, M. Barid, M. S. Hossain, S. Sen, and M. M. Azad, “Large effective area with high power fraction in the core region and extremely low effective material loss-based photonic crystal fiber (PCF) in the terahertz (THz) wave pulse for different types of communication sectors,” *Journal of Optics (India)*, vol. 50, no. 4, pp. 681–688, Dec. 2021, doi: 10.1007/s12596-021-00740-9.
- [18] S. F. Kaijage, Z. Ouyang, and X. Jin, “Porous-core photonic crystal fiber for low loss terahertz wave guiding,” *IEEE Photonics Technology Letters*, vol. 25, no. 15, pp. 1454–1457, 2013, doi: 10.1109/LPT.2013.2266412.
- [19] P. A. Agbemabiese and E. K. Akowuah, “Numerical analysis of photonic crystal fiber of ultra-high birefringence and high nonlinearity,” *Sci Rep*, vol. 10, no. 1, Dec. 2020, doi: 10.1038/s41598-020-77114-x.
- [20] H. Xu, X. Wang, Q. Kong, and D. Peng, “High numerical aperture photonic crystal fiber with silicon nanocrystals core for optical coherence tomography,” *Optik (Stuttg)*, vol. 219, Oct. 2020, doi: 10.1016/j.ijleo.2020.165000.
- [21] M. S. Islam et al., “A novel approach for spectroscopic chemical identification using photonic crystal fiber in the terahertz regime,” *IEEE Sens J*, vol. 18, no. 2, pp. 575–582, Jan. 2018, doi: 10.1109/JSEN.2017.2775642.
- [22] Z. Wu et al., “Low-loss polarization-maintaining THz photonic crystal fiber with a triple-hole core,” *Appl Opt*, vol. 56, no. 8, p. 2288, Mar. 2017, doi: 10.1364/ao.56.002288.
- [23] Md. S. Islam et al., “Zeonex-based asymmetrical terahertz photonic crystal fiber for multichannel communication and polarization maintaining applications,” *Appl Opt*, vol. 57, no. 4, p. 666, Feb. 2018, doi: 10.1364/ao.57.000666.
- [24] Y. Zhang, L. Xue, D. Qiao, and Z. Guang, “Porous photonic-crystal fiber with near-zero ultra-flattened dispersion and high birefringence for polarization-maintaining terahertz transmission,” *Optik (Stuttg)*, vol. 207, Apr. 2020, doi: 10.1016/j.ijleo.2019.163817.
- [25] J. Sultana, Md. S. Islam, K. Ahmed, A. Dinovitser, B. W.-H. Ng, and D. Abbott, “Terahertz detection of alcohol using a photonic crystal fiber sensor,” *Appl Opt*, vol. 57, no. 10, p. 2426, Apr. 2018, doi: 10.1364/ao.57.002426.
- [26] S. Dash, V. Mathur, N. Pandey, and R. K. Sinha, “Terahertz Wave Propagation Characteristics in Graded Teflon Based Solid-Core Photonic Crystal Fibre,” in *Journal of Physics: Conference Series*, Institute of Physics, 2023. doi: 10.1088/1742-6596/2426/1/012021.

- [27] B. K. Paul, M. A. Haque, K. Ahmed, and S. Sen, "A novel hexahedron photonic crystal fiber in terahertz propagation: Design and analysis," *Photonics*, vol. 6, no. 1, 2019, doi: 10.3390/PHOTONICS6010032.
- [28] M. Abdullah-Al-Shafi and S. Sen, "Design and analysis of a chemical sensing octagonal photonic crystal fiber (O-PCF) based optical sensor with high relative sensitivity for terahertz (THz) regime," *Sens Biosensing Res*, vol. 29, Aug. 2020, doi: 10.1016/j.sbsr.2020.100372.
- [29] M. M. A. Eid, M. A. Habib, M. S. Anower, and A. N. Z. Rashed, "Hollow Core Photonic Crystal Fiber (PCF)-Based Optical Sensor for Blood Component Detection in Terahertz Spectrum," *Brazilian Journal of Physics*, vol. 51, no. 4, pp. 1017–1025, Aug. 2021, doi: 10.1007/s13538-021-00906-7.
- [30] R. H. Jibon et al., "Design and numerical analysis of a photonic crystal fiber (PCF)-based flattened dispersion THz waveguide," *Opt Rev*, vol. 28, no. 5, pp. 564–572, Oct. 2021, doi: 10.1007/s10043-021-00698-w.

List of Publications

Journal paper (s):

[1] Gurmeet Singh, Shubham Sharma, Ajeet Kumar, “Analysing the Performance of Heptagonal Photonic Crystal Fibre in the Terahertz Regime”, International Conference on Design and Materials, Delhi Technological University, Delhi. This paper has been accepted for publication in the Journal of Mines, Metals & Fuels (Scopus Indexed).

[2] Gurmeet Singh, Shubham Sharma, Ajeet Kumar, “Design and Analysis of Spider-Web Photonic Crystal Fibre in the Terahertz Regime”, The European Physical Journal D. (Submitted)

Conference paper (s):

[1] Gurmeet Singh, Shubham Sharma, Ajeet Kumar, “Design and Simulation of Solid-Core Octagonal Photonic Crystal Fibre for Terahertz Wave Propagation”, Photonics 2023, Indian Institute of Sciences, Bengaluru. (Submitted)

APPENDIX 1: Thesis Plagiarism Report



Similarity Report ID: oid:27535:35581703

PAPER NAME

Thesis.pdf

AUTHOR

Gurmeet Shubham

WORD COUNT

6405 Words

CHARACTER COUNT

37131 Characters

PAGE COUNT

41 Pages

FILE SIZE

1.5MB

SUBMISSION DATE

May 17, 2023 12:57 PM GMT+5:30

REPORT DATE

May 17, 2023 12:57 PM GMT+5:30

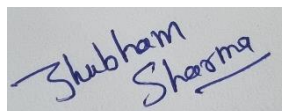
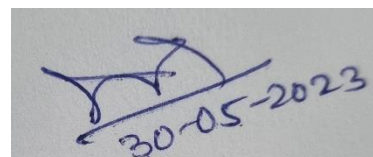
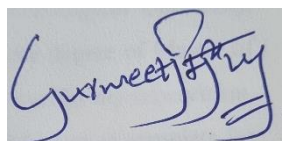
● 5% Overall Similarity

The combined total of all matches, including overlapping sources, for each database.

- 3% Internet database
- 3% Publications database
- Crossref database
- Crossref Posted Content database
- 3% Submitted Works database

● Excluded from Similarity Report

- Bibliographic material
- Small Matches (Less than 10 words)
- Manually excluded text blocks



Summary

● **5% Overall Similarity**

Top sources found in the following databases:

- 3% Internet database
- 3% Publications database
- Crossref database
- Crossref Posted Content database
- 3% Submitted Works database

TOP SOURCES

The sources with the highest number of matches within the submission. Overlapping sources will not be displayed.

1	dspace.dtu.ac.in:8080 <small>Internet</small>	<1%
2	Md. Ibrahim, Chinmoy Das, Md. Tabil Ahammed, Niranjon Biswas et al. ... <small>Crossref</small>	<1%
3	Lavanya A., G. Geetha. "A novel hybrid hexagonal photonic crystal fibre... <small>Crossref</small>	<1%
4	lib.buet.ac.bd:8080 <small>Internet</small>	<1%
5	nature.com <small>Internet</small>	<1%
6	Md. Abdullah-Al-Shafi, Nasima Akter, Shuvo Sen, Md. Selim Hossain. "... <small>Crossref</small>	<1%
7	Md. Anwar Sadath, Md. Muhaiminur Rahman, Mohammad Saiful Islam,... <small>Crossref</small>	<1%
8	Akash Bosu, Md. Rabiul Hasan, Sanjida Akter, Shumaia Sharmin. "Desi... <small>Crossref</small>	<1%

Sources overview

9	University of Birmingham on 2016-04-01 Submitted works	<1%
10	curve.carleton.ca Internet	<1%
11	Bikash Kumar Paul, Kawsar Ahmed, Vigneswaran Dhasarathan, Fahad ... Crossref	<1%
12	Chuan Shi Ang, Abdul Mu'iz Maidi, Shubi Kaijage, Feroza Begum. "Highl... Crossref	<1%
13	VIT University on 2014-12-10 Submitted works	<1%
14	core.ac.uk Internet	<1%
15	ijeecs.iaescore.com Internet	<1%
16	Bikash Kumar Paul, Touhid Bhuiyan, Lway Faisal Abdulrazak, Kaushik ... Crossref	<1%
17	Izaddeen K. Yakasai, Pg Emeroylariffion Abas, Hazwani Suhaimi, Feroz... Crossref	<1%
18	Jingxuan Yang, Wei Li. "Design for Terahertz Circular-Core Photonic Cr... Crossref	<1%
19	Md. Abdullah-Al-Shafi, Shuvo Sen. "Design and analysis of a chemical ... Crossref	<1%
20	University of Asia Pacific on 2021-06-05 Submitted works	<1%

Sources overview

21	University of Nottingham on 2011-07-29 Submitted works	<1%
22	baadalsg.inflibnet.ac.in Internet	<1%
23	bdigital.unal.edu.co Internet	<1%
24	epdf.tips Internet	<1%

● **Excluded from Similarity Report**

- Bibliographic material
- Manually excluded text blocks
- Small Matches (Less than 10 words)

EXCLUDED TEXT BLOCKS

A DISSERTATIONSUBMITTED IN PARTIAL FULFILLMENT OF THE

dspace.dtu.ac.in:8080

Under the supervision of(Dr

dspace.dtu.ac.in:8080

students of M.Sc. Physics hereby

dspace.dtu.ac.in:8080

which is submitted by us to the Department of Applied Physics,Delhi Technologica...

dspace.dtu.ac.in:8080

DEPARTMENT OF APPLIED PHYSICSDELHI TECHNOLOGICAL UNIVERSITY(Forme...

dspace.dtu.ac.in:8080

Department of Applied Physics, Delhi Technological University,Delhi, in partial

dspace.dtu.ac.in:8080

University for providing

Pathfinder Enterprises on 2023-04-30

would also like to thank

doras.dcu.ie

would like to extend

Westminster International University in Tashkent on 2023-03-10

Declarationii...

dspace.dtu.ac.in:8080

Excluded from Similarity Report

ANALYSING THE PERFORMANCE OF HEPTAGONAL PHOTONIC CRYSTAL FIBRE IN THE TERAHERTZ REGIME

Gurmeet Singh, Shubham Sharma, Ajeet Kumar (✉)

Advanced Photonics Simulation Research Laboratory, Department of Applied Physics, Delhi Technological University, Bawana Road, New Delhi, Delhi 110042, India (Email: ajeetdph@dtu.ac.in, ajeetdph@gmail.com)

ABSTRACT: We designed a heptagonal cladding (HC) solid-core (SC) photonic crystal fibre (PCF) to improve the performance in the terahertz (THz) regime. The effective material loss, confinement loss, effective mode area, and nonlinear coefficient have culminated using Chalcogenide glass (ChGs) material as a core because it provides high optical transparency in the infrared region. The air holes in the cladding region give stability to the PCF that can work on the principle of total internal reflection (TIR). The terahertz frequency range from 0.3 to 4 THz has been used to understand the confinement of infrared waves in the fibre. From existing results, confinement loss is reported as 10^{-9} dB/cm, which is reported as low as 10^{-15} dB/cm in the proposed design while varying air filling fraction (AFF) and THz frequency individually. Using COMSOL Multiphysics software, all the results are computed using computational electromagnetics, whose finite element method (FEM) is performed. With an appropriate choice of parameters, the losses can be minimised.

Index Terms: *Heptagonal cladding photonic crystal fibre, Terahertz, Confinement loss, and Effective material loss.*

1. Introduction

The 0.1–10 THz range of electromagnetic waves is called terahertz radiation, sometimes called submillimetre – wave radiation [1]. These frequencies are lower than infrared lights but higher than radio waves and microwaves. The terahertz (THz) frequency can be used to develop the field of discreet imaging [2], astronomy [3], drug censoring [4], spectroscopy [5], DNA hybridisation [6] and sensors [7], communications [8], etc. Other medical areas of diagnostics, such as skin cancer, breast

cancer, and other critical diseases [2], have been used for the radiation of terahertz (THz) ranges.

Photonic crystal fibre (PCF), a micro-structured fibre, has been introduced in THz wave propagation. These unique fibres have hollow, porous, and solid cores that can confine light and light captivity features that are impossible with conventional optical fibre. Some of these PCFs' special features are low material loss and confinement loss, high effective mode area, birefringence, and sensitivity. The hollow core fibre that uses photonic band gap characteristics for waveguiding is based on photonic crystals. Significant amounts of the THz field propagate in the air in this fibre. The solid core of PCF works on total internal reflection (TIR). The centre of these fibres transmits the most significant amount of wave energy. Terahertz communication devices use Topas and Zeonex materials as their applications, too [9].

Many studies have used terahertz (THz) waveguides to describe and briefly analyse the design and performance of PCF structures. A chemical molecule known as a chalcogenide comprises an anion of chalcogen and one additional electropositive element. Materials based on chalcogenides, such as those made of telluride, selenide, and sulphide, are widely available. In various fields, including photovoltaic, photocatalyst, sensor, fuel cell, and battery, binary, ternary, and quaternary chalcogenide materials are helpful. For mid-wave-infrared (MWIR) fibres made of non-oxide components, chalcogenide glasses (ChGs) are an appealing option since they have optical transparency in both the mid- and long-wave infrared ranges [10].

HC PCF results are compared to the existing results from Ref. [11] comprising effective material loss, confinement loss, and effective mode area, which are 8.0×10^{-2} dB/cm, 3.20×10^{-13} dB/cm, and 1.0×10^{-7} m², Ref. [12] talks about the same values, i.e., effective material loss, confinement loss, and effective mode area which are 5.0×10^{-2} dB/cm, 7.79

$\times 10^{-12}$ dB/cm, and 2.0×10^{-5} m². Reference [13] is mentioned a slightly different parameter; in place of effective material loss, it talks about the nonlinearity coefficient, confinement loss, and effective mode area, which are 3.0×10^{-8} rad/Wm, 10^{-9} dB/cm, and 5.62×10^{-6} m².

In this paper, we have simulated the PCF using the finite element method. Four results are evaluated: EML, confinement loss, effective mode area, and nonlinearity coefficient.

2. Proposed heptagonal PCF design

The proposed design of HC SC PCF is shown in Fig. 1, which shows the transverse cross-sectional view of the fibre. Five layers of heptagonal shape have been used to build this fibre in which numbers of air holes in the 1st, 2nd, 3rd, 4th, and 5th layers are 7, 14, 21, 28, and 35, respectively, introduced in the cladding region with different material.

In this design, chalcogenide glass which has

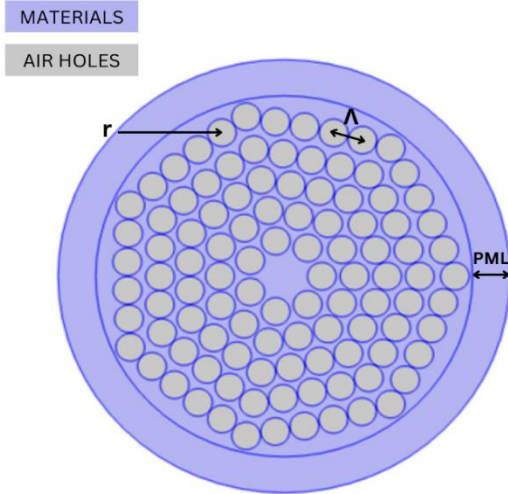


Fig. 1. Proposed HC SC PCF

various applications in the infrared region has been used. The distance between two air holes is known as pitch; using it, the air filling fraction (AFF) remains the same when the frequency varies in the range of 0.3 – 4.0 THz. At 1 THz of frequency, AFF goes between 0.4 to 0.6.

The confinement loss is also calculated using the perfectly matched layer.

3. Formulations

The effective material loss (EML) or absorption loss (α_{eff}) can be calculated as

$$\alpha_{\text{eff}} = \sqrt{\frac{\epsilon_0}{u_0}} \frac{\int_{\text{mat}} n_{\text{mat}} \alpha_{\text{mat}} |E|^2 dA}{2 |\int_{\text{all}} s_z dA|} \left(\frac{dB}{cm} \right) \quad (1)$$

Where α_{mat} is the bulk material loss, \vec{s}_z is the pointing vector in the z-direction.

Confinement loss which is the loss in a perfectly matched layer (PML), can be evaluated as

$$L \left[\frac{dB}{cm} \right] = \frac{40 \pi}{\ln(10)\lambda} \text{Im}(n_{\text{eff}}) \times 10^{-2} \\ = 8.686 k_0 \text{Im}(n_{\text{eff}}) \times 10^{-2} \quad (2)$$

Where $\text{Im}(n_{\text{eff}})$ is the complex part of the fundamental mode.

A more effective mode area will make a better PCF which can be calculated using [11],

$$A_{\text{eff}} = \frac{[\int I(r) dr]^2}{[\int I^2(r) dr]} \quad (3)$$

The nonlinear coefficient, which must be less for the highly effective mode area, can be simulated as

$$\gamma = \left(\frac{2\pi}{\lambda} \right) \left(\frac{n_2}{A_{\text{eff}}} \right) \quad (4)$$

Where n_2 is the nonlinear refractive index [12].

4. Numerical results

Using the FEM, we have culminated the effective material loss, confinement loss, effective mode area, and nonlinear coefficient for the given structure. Chalcogenide glass with a refractive index of 2.65 is used to get desired results.

Initially, to get results to vary frequency in the range of 0.3 to 4 THz, the fixed parameters have been used, such as radius of air holes, $r = 0.57$ mm,

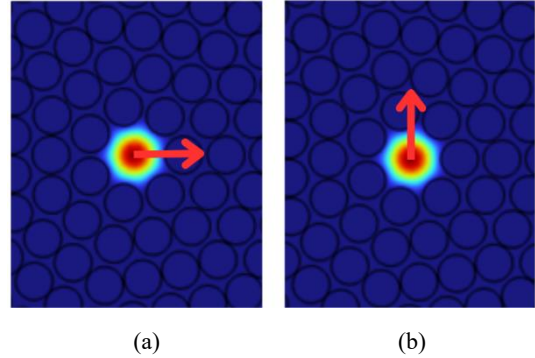


Fig. 2. Fundamental Mode at 1 THz for (a) x-polarization, and (b) y-polarization.

$\Lambda = 1.9$ mm, cladding = 7.5 mm, and 20% of cladding as PML. Then, the diameter/pitch ratio, also known as air filling fraction (AFF), ranging from 0.4 to 0.6, is used to see the effect on the confinement loss. Figure 2 shows the contour plot of the field intensity for the x-polarization and y-polarization at 1 THz (fundamental mode = 2.60).

Figure 3 depicts effective material loss (EML) variation against the varying frequency. The EML reported as low as 1.28×10^{-2} dB/cm at 0.3 THz and 1.29×10^{-2} at 4.0 THz. The EML reaches absorption loss at a higher frequency but remains under the value for the lower one.

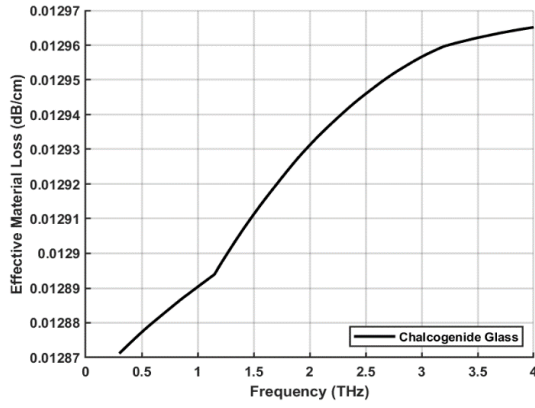


Fig. 3. Variation of EML with frequency.

The negligible confinement loss is obtained with 20 % extra cladding used as PML. It is reported 3.91×10^{-15} dB/cm at 0.3 THz and 4.06×10^{-13} dB/cm at 4.0 THz. This is due to better radiation confinement

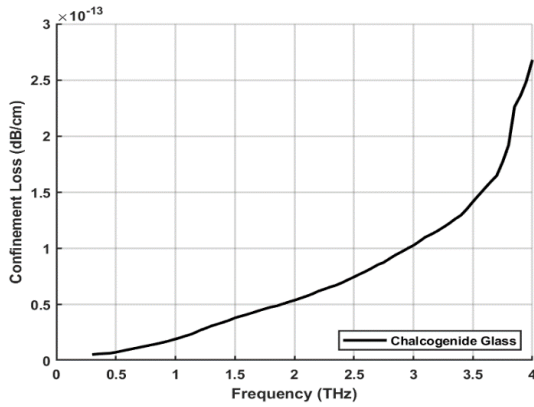


Fig. 4. Variation of confinement loss with

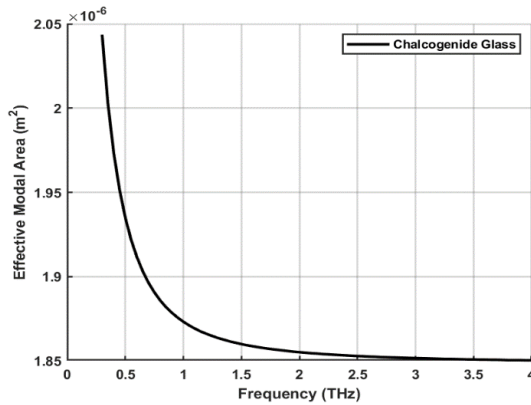


Fig. 5. Variation of effective mode area with frequency.

in the infrared region by Chalcogenide Glass and high AFF near the core. Figure 4 shows its variation with frequency. The effective mode area is simulated with a very high value of 2.04×10^{-6} m² at the lowest frequency of 0.3 THz. According to the variation shown in Fig. 5, it goes down to 1.85×10^{-6} m² at 4.0 THz because wave energy increases with frequency.

Nonlinearity losses become low for high effective mode area, which can be seen by

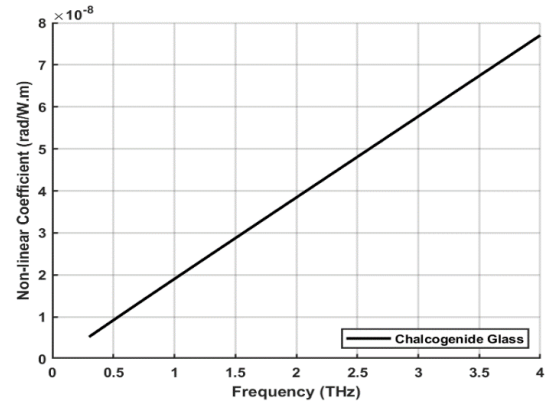


Fig. 6. Variation of γ with frequency.

comparing Figures 5 and 6. The nonlinearity coefficient is 5.23×10^{-9} rad/Wm at 0.3 THz and becomes maximum when the effective mode area is low. This is due to the low energy entering the fibre's core at a lower frequency.

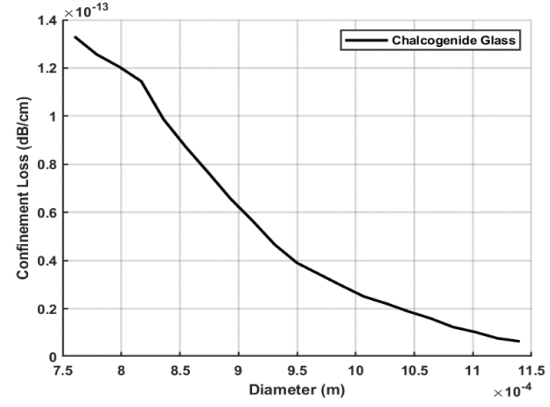


Fig. 7. Variation of Confinement Loss with Diameter of air holes.

Figure 7 depicts the variation of confinement loss with diameter/pitch ratio, also known as AFF, ranging from 0.4 to 0.6, making the diameter of air holes from 7.6×10^{-4} m to 1.14×10^{-3} m. The confinement loss is high for lower AFF, i.e., 1.68×10^{-13} dB/cm for 0.4 and decreases to 5.36×10^{-15} dB/cm for 0.6.

Table – 1 relates existing results [12 – 14] and simulated results of HC SC PCF in this paper.

5. Conclusion

In conclusion, the solid core PCF with very low confinement loss and high effective mode area is proposed for THz wave propagation. The HC SC PCF performance has improved using the chalcogenide glass as the core material. In the broad range of THz from 0.3 to 4.0 THz, the effective material loss lower of 1.28×10^{-2} dB/cm and confinement loss 3.91×10^{-15} dB/cm could be achieved. High-effective mode area can help make this PCF reliable; hence, it can be used for various applications such as communications, spectroscopy, etc.

Table 1. Proposed HC SC PCF with the existing designs.

Ref.	EML (dB/cm)	L (dB/cm)	A_{eff} (m ²)	γ (rad/Wm)
[11]	8.0×10^{-2}	3.20×10^{-13}	1.0×10^{-7}	-
[12]	5.0×10^{-2}	7.79×10^{-12}	2.0×10^{-5}	-
[13]	-	10^{-9}	5.62×10^{-6}	3.0×10^{-8}
Proposed design	1.28×10^{-2}	3.91×10^{-15}	2.04×10^{-6}	5.23×10^{-9}

References

- [1] Islam, Md Saiful, Jakeya Sultana, Alex Dinovitser, Mohammad Faisal, Mohammad Rakibul Islam, Brian W-H. Ng, and Derek Abbott. "Zeonex-based asymmetrical terahertz photonic crystal fiber for multichannel communication and polarization maintaining applications." *Applied optics* 57, no. 4 (2018): 666-672.
- [2] Chen, Q., Zhiping Jiang, G. X. Xu, and X-C. Zhang. "Near-field terahertz imaging with a dynamic aperture." *Optics letters* 25, no. 15 (2000): 1122-1124.
- [3] Ho, Louise, Michael Pepper, and Philip Taday. "Signatures and fingerprints." *Nature Photonics* 2, no. 9 (2008): 541-543.
- [4] Strachan, Clare J., Philip F. Taday, David A. Newnham, Keith C. Gordon, J. Axel Zeitler, Michael Pepper, and Thomas Rades. "Using terahertz pulsed spectroscopy to quantify pharmaceutical polymorphism and crystallinity." *Journal of pharmaceutical sciences* 94, no. 4 (2005): 837-846.
- [5] Zhang, Jiangquan, and D. Grischkowsky. "Waveguide terahertz time-domain spectroscopy of nanometer water layers." *Optics letters* 29, no. 14 (2004): 1617-1619.
- [6] Nagel, M., P. Haring Bolivar, M. Brucherseifer, H. Kurz, A. Bosserhoff, and R. Büttner. "Integrated THz technology for label-free genetic diagnostics." *Applied Physics Letters* 80, no. 1 (2002): 154-156.
- [7] Jamison, S. P., R. W. McGowan, and D. Grischkowsky. "Single-mode waveguide propagation and reshaping of sub-ps terahertz pulses in sapphire fibers." *Applied physics letters* 76, no. 15 (2000): 1987-1989.
- [8] Jin, Yun-Sik, Geun-Ju Kim, and Seok-Gy Jeon. "Terahertz dielectric properties of polymers." *Journal of the Korean Physical Society* 49, no. 2 (2006): 513.
- [9] Abdullah-Al-Shafi, Md, Nasima Akter, Shuvo Sen, and Md Selim Hossain. "Design and performance analysis of background material of zeonex based high core power fraction and extremely low effective material loss of photonic crystal fiber in the terahertz (THz) wave pulse for many types of communication areas." *Optik* 243 (2021): 167519.
- [10] Yakasai, Izaddeen K., Pg Emeroylariffion Abas, Sharafat Ali, and Feroza Begum. "Modelling and simulation of a porous core photonic crystal fibre for terahertz wave propagation." *Optical and Quantum Electronics* 51 (2019): 1-16.
- [11] Zhang, Yani, Lu Xue, Dun Qiao, and Zhe Guang. "Porous photonic-crystal fiber with near-zero ultra-flattened dispersion and high birefringence for polarization-maintaining terahertz transmission." *Optik* 207 (2020): 163817.
- [12] Sultana, Jakeya, Md Saiful Islam, Kawsar Ahmed, Alex Dinovitser, Brian W-H. Ng, and Derek Abbott. "Terahertz detection of alcohol using a photonic crystal fiber sensor." *Applied optics* 57, no. 10 (2018): 2426-2433.
- [13] Dash, Shikhar, Varun Mathur, Nilesh Pandey, and Ravindra K. Sinha. "Terahertz Wave Propagation Characteristics in Graded Teflon Based Solid-Core Photonic Crystal Fibre." In *Journal of Physics: Conference Series*, vol. 2426, no. 1, p. 012021. IOP Publishing, 2023.

PAPER ACCEPTANCE MAIL



Gurmeet Singh 2K21/MSCPHY/15 <gurmeetsingh_2k21mscphy15@dtu.ac.in>

ICDM-2023 notification for paper 39

1 message

ICDM-2023 <icdm2023-0@easychair.org>

Sat, Apr 29, 2023 at 5:02 PM

To: Gurmeet Singh <gurmeetsingh_2k21mscphy15@dtu.ac.in>

Dear Authors,

I am pleased to inform you that now reviewers have commented on your manuscript, and your manuscript has been recommended for consideration for publication in the Journal of Mines, Metals & Fuels (Scopus Indexed)

You are advised to revise your manuscript as per the comments of the reviewer (given below to this mail) and submit the editable doc file of the manuscript in the attached format by May 5, 2023, to the conference through the google form,

<https://forms.gle/UqAGgzBNDf24afH47>

You are further advised to register for the conference by paying the registration fee through the following link, which is valid until May 5, 2023:

<https://pages.razorpay.com/icdm2023>

Registration Fee for Indian Delegates is 10000 INR

Authors are advised to submit the revised paper and register within stipulated deadlines to contribute for timely publication of papers.

Looking for your presence to make ICDM-2023 a huge success.

Regards
Chairman,
ICDM-2023

SUBMISSION: 39

TITLE: Analysing The Performance Of Heptagonal Photonic Crystal Fibre In The Terahertz Regime

----- REVIEW 1 -----

SUBMISSION: 39

TITLE: Analysing The Performance Of Heptagonal Photonic Crystal Fibre In The Terahertz Regime

AUTHORS: Gurmeet Singh, Shubham Sharma and Ajeet Kumar

----- Overall evaluation -----

SCORE: 3 (strong accept)

----- TEXT:

THE PAPER IS WELL WRITTEN THE AUTHOR ARE SUGGESTED TO ADD SOME MORE DISCUSSION IN THE RESULT SECTION. MOREOVER, THE AUTHORS ARE ALSO SUGGESTED TO CHECK FOR THE TYPOS AND GRAMMATICAL ERRORS.

It would be Great if the authors can add more articles IN THE literature, the articles should be recent and relevant to the work done by the author.

REGISTRATION STATUS

TECHNOSCIENCE

GSTIN - 09AKCPA7681H1Z3

Payment Receipt Transaction Reference: pay_Lr3EHsAIF2JfSd

This is a payment receipt for your transaction on ICDM-2023

AMOUNT PAID ₹ 10,000.00

ISSUED TO
gurmeetsingh_2k21mscphy15@dtu.ac.in
+918130686073

PAID ON
18 May 2023

DESCRIPTION	UNIT PRICE	QTY	AMOUNT
Amount	₹ 10,000.00	1	₹ 10,000.00
Total			₹ 10,000.00
Amount Paid			₹ 10,000.00

INDEXING

INFORMATICS JOURNAL 5 **Journal of Mines, Metals and Fuels** Register Login
Print ISSN : 0022-2755
Publishers' Informatics Publishing Limited and Books & Journals Private Ltd.

HOME ABOUT THE JOURNAL CURRENT ARCHIVES EDITORIAL TEAM PUBLICATION FEES ONLINE FIRST Q SEARCH

HOME / Abstracting and Indexing

Abstracting and Indexing

Listed below are a few. This ensures there is a wider visibility to articles published in our Journal.

- SCOPUS
- UdiEdge
- EBSCO
- UGC





Submit a Manuscript

AUTHORS CORNER

- Instructions to Authors
- Publication Fees
- Indexing/Abstracting
- Journal Policies and Ethics
- CrossMark Policy
- Information for Reviewers
- Submission Process
- Pre-submission checklist

EDITORIAL TEAM

Managing Editor & Publisher
P K Chanda

DESIGN AND SIMULATION OF SOLID-CORE OCTAGONAL PHOTONIC CRYSTAL FIBRE FOR TERAHERTZ WAVE PROPAGATION

Gurmeet Singh, Shubham Sharma, and Ajeet Kumar (✉)

Advanced Photonics Simulation Research Laboratory, Department of Applied Physics, Delhi Technological University, Bawana Road, New Delhi, Delhi 110042, India (Email: ajeetdph@dtu.ac.in)

ABSTRACT: A solid-core (SC) octagonal photonic crystal fibre (O-PCF) that operates in a terahertz regime has been designed to improve its performance. The effective material loss (EML), confinement loss, effective mode area, and nonlinear coefficient have been investigated and compared of two different media, i.e., silica glass and Teflon. The terahertz frequency from 0.7 to 3.0 THz has been used to analyse all the results using a full-vectorial finite element method (FEM) for which COMSOL Multiphysics software is used. With a suitable choice of parameters, the proposed SC O-PCF can minimise losses and increase the effective mode area of the fundamental mode.

Index Terms – Solid core photonic crystal fibre, terahertz, effective material loss, confinement loss, effective mode area.

1. INTRODUCTION

Photonic crystal fibres (PCFs), or holy fibres, are made of a single material with numerous air holes in cladding that remain intact periodically [1]. Low index cladding around the core helps tune dispersion slope and control confinement losses [2]. As per the guiding mechanism, PCFs are characterised in two ways: one which has a solid core and a low index in the cladding region that makes PCFs work like a conventional fibre because this guides light by total internal reflection (TIR) [3 – 4], and photonic band gap (PBG) guidance PCF is another type which is equipped to control the light guidance for any frequency band. PCFs have many applications, such as PCF-based sensors, mid- and far-infrared guidance, terahertz guidance, and so on [5].

The communication sector has recently evolved and seen tremendous changes [6]. The recent change has come with various applications in the terahertz (THz) region. On the electromagnetic spectrum, terahertz has a frequency range from 100 GHz to 10

THz, in which phonons, excitons, and cooper pairs are important material parameters that make terahertz frequency a vital region [7].

The design of O-PCF can be obtained by arranging air holes based on an isosceles triangle of $\pi/4$ vertices angle. The arrangement of five rings can be formed, and by rotating the triangle with periods of $\pi/4$, $\pi/2$, $3\pi/4$, π , $5\pi/4$, $3\pi/2$, and $7\pi/4$ the octagonal design is obtained [1]. In this design, the finite element method (FEM) has been applied because, using this, we can approach continuous functions as discrete models [8].

In the existing PCFs design, Ref. [9] reported for hexagonal PCF (H-PCF), in which at 1 THz confinement loss, effective mode area, and nonlinearity coefficient are 10^{-9} dB/cm, 5.62×10^{-6} m², and 3×10^{-8} , respectively. Ref. [10] reported EML, confinement loss, and effective mode area of 6.6×10^{-2} /cm, 5.42×10^{-13} /cm, and 1.1×10^{-7} m². Moreover, in Ref. [11], oligoporous – core (PC) PCF at 1 THz confinement loss, EML, and effective area are 7.24×10^{-7} /cm, 6.27×10^{-2} /cm, 9.5×10^{-6} m².

In this paper, we have investigated the required parameters in the THz regime from 0.7 THz to 3 THz. We examined minimum losses and the maximum effective area for fused silica glass and Teflon materials. This paper is organised so that in section 2, we introduce the geometrical structure of SC O-PCF and related parameters. Then in section 3, required formulations are presented, and in sections 4 and 5, numerical results and conclusions are reported.

2. PROPOSED SOLID CORE PCF DESIGN

Figure 1 shows the transverse cross-sectional view of the proposed SC O-PCF. The octagonal five layers array of air holes is built in another material along the length of the fibre. Air holes in the 1st, 2nd, 3rd, 4th, and 5th layers are 8, 16, 24, 32, and 40, respectively, introduced in the cladding region.

For the comparison, two different media, i.e., Fused Silica and Teflon, are used. In all five rings,

the radius is constant throughout. The distance between two air holes is the pitch Λ , and the diameter/pitch ratio, i.e., air filling fraction (AFF), is fixed at 0.5. The diameter of air holes and pitch remains constant throughout the simulation study.

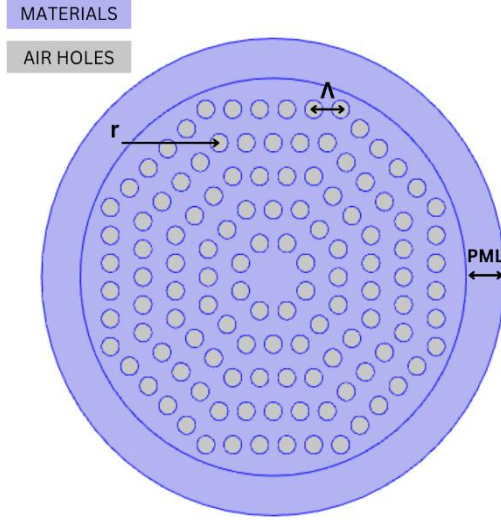


Fig. 1. Proposed SC O-PCF

The perfectly matched layer is also used to calculate the confinement loss.

3. FORMULATIONS

The COMSOL Multiphysics software, based on a full-vectorial finite element method (FEM), evaluates the effective indices, confinement loss, and nonlinear coefficient. Absorption loss or EML (α_{eff}) depicts the loss of the PCFs while operating at THz frequencies, and it can be calculated as [12]

$$\alpha_{eff} = \frac{\sqrt{\frac{\epsilon_0}{u_0}} \int_{mat} n_{mat} \alpha_{mat} |E|^2 dA}{2 \int_{all} s_z dA} \left(\frac{dB}{cm} \right) \quad (1)$$

Where α_{mat} is the material absorption loss, $\vec{s}_z = \frac{1}{2} (\vec{E} \times \vec{H}) \hat{z}$ is the pointing vector of the z - component, here, E and H are electric and magnetic fields.

Confinement loss which is essential to find in terahertz applications of PCF, can be evaluated from the imaginary value of n_{eff} as

$$\begin{aligned} L \left[\frac{dB}{cm} \right] &= \frac{40 \pi}{\ln(10) \lambda} \text{Im}(n_{eff}) \times 10^{-2} \\ &= 8.686 k_0 \text{Im}(n_{eff}) \times 10^{-2} \end{aligned} \quad (2)$$

Where $\text{Im}(n_{eff})$ is the imaginary part of the effective mode index of that mode. And $k_0 = \frac{2\pi}{\lambda}$; λ is the operating wavelength of light in meters [13].

In high-power transmission, PCFs with a large effective mode area are used. This characteristic also suppresses the unwanted nonlinear effects. A greater

effective mode area will give lesser nonlinear effects and vice versa. It is calculated using [14]

$$A_{eff} = \frac{[\int I(r) dr]^2}{[\int I^2(r) dr]} \quad (3)$$

where $I(r) = [E(t)]^2$ is the amplitude of the transverse electric field propagating through the fibre.

The nonlinear coefficient defines the interaction of the nonlinearity of light with an optical material. It can be found by

$$\gamma = \left(\frac{2\pi}{\lambda} \right) \left(\frac{n_2}{A_{eff}} \right) \quad (4)$$

Where n_2 is the nonlinear refractive index of the material [15].

4. NUMERICAL RESULTS

We have investigated the effective material loss, confinement loss, effective mode area, and nonlinear coefficient using a full vectorial finite element method (FEM) in the given structure. To correlate, fused silica and Teflon of refractive indices 1.45 and 1.38, respectively, have been used.

Initially, we have chosen the fixed structural parameters, $r = 0.95 \text{ mm}$, $\Lambda = 1.9 \text{ mm}$, $cladding = 10.4 \text{ mm}$, and outer layer 20% of cladding as PML. The fundamental modes at 1 THz frequency are observed for fused silica and Teflon, which are 1.44 and 1.37, respectively. Figure 2 shows the contour plot of the field intensity of one of the fundamental modes.

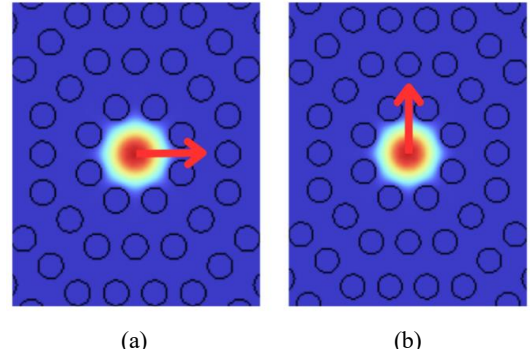


Fig. 2. Fundamental Mode of Fused Silica at 1 THz in (a) x-polarization, and (b) y-polarization.

Figure 3 (a) shows the variation in the effective material loss for increasing frequency when the core-cladding media is set to fused silica. The integration of the numerator of (1) is performed only over the solid material region, which indents EML as a function of frequency. The loss is reported as low as $2.07 \times 10^{-2} \text{ dB/cm}$ at 0.7 THz of frequency and reached as high as $2.08 \times 10^{-2} \text{ dB/cm}$ at 3 THz. In Figure 3 (b), a similar situation is observed where Teflon made a solid material, but here losses are

slightly more significant because of high bulk material absorption loss.

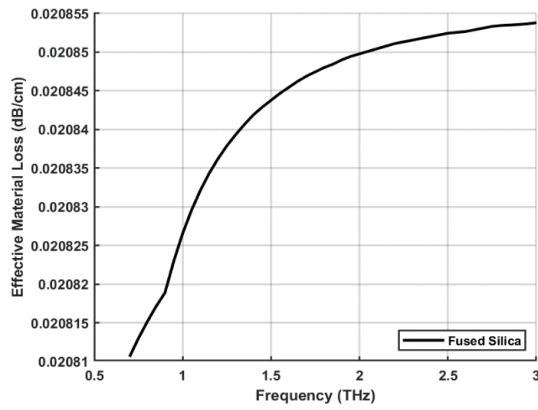


Fig. 3 (a). Variation of EML of Fundamental Mode with frequency (fused silica).

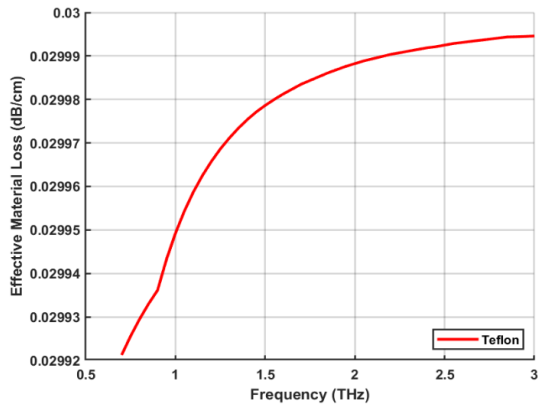


Fig. 3 (b). Variation of EML of Fundamental Mode with frequency (Teflon).

Figure 4 is the comparison of confinement loss between fused silica and Teflon. Confinement loss is directly dependent on the frequency clarifies that at a lower frequency of 0.7 THz, it approximates zero but increases to 10^{-15} dB/cm for both materials in fundamental mode; however, Teflon is slightly reliable for containing the light within the domain.

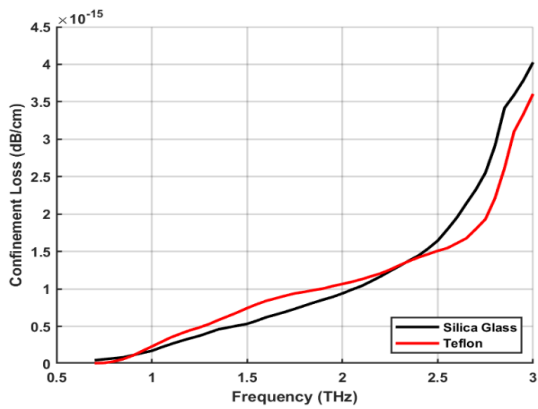


Fig. 4. Variation of L of Fundamental Mode with frequency (silica glass and Teflon).

In Figure 5, large effective mode areas are obtained for lower frequencies in fundamental

modes; however, it gradually decreases with an increase in frequency. Teflon shows a large effective mode area within the range [0.7, 3.0] THz in both materials.

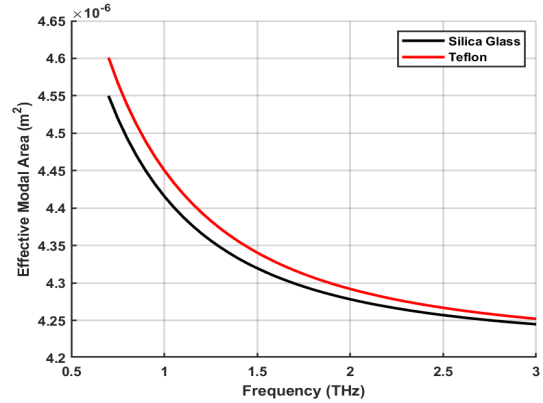


Fig. 5. Variation of effective mode area of Fundamental Mode with frequency (silica glass and Teflon).

Theoretically, a low nonlinear coefficient will be obtained with a larger effective mode area. Figure 6 can prove the theory; at lower frequencies, nonlinear coefficients are as low as 10^{-10} rad/W.m for both media, and it keeps increasing with an increase in frequency. Yet Teflon is the most effective compared to silica glass because of its high value of the nonlinear refractive index, which is 3.2×10^{-6} .

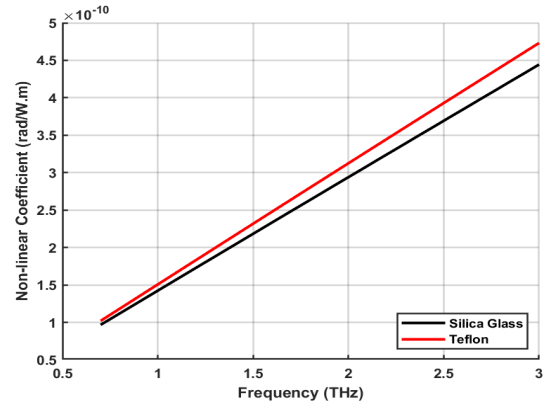


Fig. 6. Variation of γ of Fundamental Mode with frequency (silica glass and Teflon).

Table – 1 compares previous results [9 – 11] and determined results of SC O-PCF in this paper. The proposed design shows better results in comparison to other existing models.

5. CONCLUSION

In the proposed O-PCF, we have improved the required factors by changing the AFF in the cladding region. Making all five rings uniform plays a vital role and using materials like fused silica and Teflon reported low EML and confinement loss due to their low material absorption loss.

This paper obtains the fundamental mode of fused silica and Teflon at 1.44 and 1.37.

Table 2. Feature of proposed SC O – PCF with the previous designs.

Ref.	EML (dB/cm)	L (dB/cm)	A_{eff} (m ²)	γ (rad/Wm)
[9]	-	10^{-9}	5.62×10^{-6}	3.0×10^{-8}
[10]	6.60×10^{-2}	5.42×10^{-13}	1.10×10^{-7}	-
[11]	5.0×10^{-2}	7.24×10^{-7}	9.50×10^{-6}	-
Proposed (fused silica)	2.08×10^{-2}	1.66×10^{-16}	4.42×10^{-6}	1.42×10^{-10}
Proposed (Teflon)	2.99×10^{-2}	2.83×10^{-16}	4.45×10^{-6}	1.51×10^{-10}

Both materials can reduce EML up to $5 - 6 \times 10^{-2}$ dB/cm by simulating the value for fused silica 2.08×10^{-2} dB/cm and Teflon 2.99×10^{-2} dB/cm. Moreover, confinement losses are reduced from 10^{-13} to 10^{-16} dB/cm with the proposed design. This design will be helpful in several applications such as telecommunication, spectroscopy, sensing, etc.

REFERENCES

- [1] Chiang, J. S., & Wu, T. L. (2006). Analysis of propagation characteristics for an octagonal photonic crystal fiber (O-PCF). *Optics Communications*, 258(2), 170-176.
- [2] Habib, M. S., Habib, M. S., Razzak, S. A., & Hossain, M. A. (2013). Proposal for highly birefringent broadband dispersion compensating octagonal photonic crystal fiber. *Optical Fiber Technology*, 19(5), 461-467.
- [3] Ademgil, H. (2014). Highly sensitive octagonal photonic crystal fiber based sensor. *Optik*, 125(20), 6274-6278.
- [4] Ahmed, K., & Morshed, M. (2016). Design and numerical analysis of microstructured-core octagonal photonic crystal fiber for sensing applications. *Sensing and Bio-Sensing Research*, 7, 1-6.
- [5] Cerqueira, S. A. (2010). Recent progress and novel applications of photonic crystal fibers. *Reports on progress in physics*, 73(2), 024401.
- [6] Hossain, M. S., Sen, S., & Hossain, M. M. (2021). Performance analysis of octagonal photonic crystal fiber (O-PCF) for various communication applications. *Physica Scripta*, 96(5), 055506.
- [7] Goto, M., Quema, A., Takahashi, H., Ono, S., & Sarukura, N. (2004). Teflon photonic crystal fiber as terahertz waveguide. *Japanese Journal of Applied Physics*, 43(2B), L317.
- [8] Tekkaya, A. E., & Soyarslan, C. (2018). Finite Element Method. *The International Academy for Production Engineering*; Laperrière, L., Reinhart, G., Eds.
- [9] Dash, S., Mathur, V., Pandey, N., & Sinha, R. K. (2023, February). Terahertz Wave Propagation Characteristics in Graded Teflon Based Solid-Core Photonic Crystal Fibre. In *Journal of Physics: Conference Series* (Vol. 2426, No. 1, p. 012021). IOP Publishing.
- [10] Kumar Paul, B., Haque, M. A., Ahmed, K., & Sen, S. (2019, March). A novel hexahedron photonic crystal fiber in terahertz propagation: design and analysis. In *Photonics* (Vol. 6, No. 1, p. 32). MDPI.
- [11] Islam, M. S., Sultana, J., Dinovitser, A., Ng, B. W. H., & Abbott, D. (2018). A novel Zeonex based oligoporous-core photonic crystal fiber for polarization preserving terahertz applications. *Optics Communications*, 413, 242-248.
- [12] Rana, S., Ali, S., Ahmed, N., Islam, R., & Aljunid, S. A. (2016). Ultra-high birefringent and dispersion-flattened low loss single-mode terahertz wave guiding. *IET Communications*, 10(13), 1579-1583.
- [13] Saitoh, K., Koshiba, M., Hasegawa, T., & Sasaoka, E. (2003). Chromatic dispersion control in photonic crystal fibers: application to ultra-flattened dispersion. *Optics express*, 11(8), 843-852.
- [14] Hassani, A., Dupuis, A., & Skorobogatiy, M. (2008). Low loss porous terahertz fibers containing multiple subwavelength holes. *Applied Physics Letters*, 92(7), 071101.
- [15] Eid, M. M., Habib, M. A., Anower, M. S., & Rashed, A. N. Z. (2021). Highly sensitive nonlinear photonic crystal fiber based sensor for chemical sensing applications. *Microsystem Technologies*, 27, 1007-1014.

INDEXING

Abstracted and indexed in

DBLP
EI Compendex
INSPEC

Japanese Science and Technology Agency (JST)
SCImago
SCOPUS

WTI Frankfurt eG
zbMATH

Design and analysis of spider–web photonic crystal fibre in the terahertz regime

Gurmeet Singh, Shubham Sharma, and Ajeet Kumar*

Advanced Photonics Simulation Research Laboratory, Department of Applied Physics, Delhi Technological University, Bawana Road, New Delhi, Delhi 110042, India (*ajeetdph@dtu.ac.in, ajeetdph@gmail.com)

Abstract: A newly formed spider-web (SW) photonic crystal fibre (PCF) having a solid core has been designed. The finite element method (FEM) has been used to investigate the guiding properties in the terahertz radiation ranging from 0.1 to 3.0 THz frequency. All numerically simulated results of different optical parameters have shown low confinement loss and low effective material loss (EML). The high core power fraction of 99% and the effective mode area of $1.06 \times 10^{-5} m^2$ make this fibre an exception. Moreover, V-parameter has also been calculated to check the mode of the fibre. The proposed design is a fundamental or mono–mode SW – PCF convenient for broadband transmission and other terahertz applications.

Index terms: Photonic crystal fibre, terahertz, confinement loss, effective material loss, effective mode area.

1. Introduction

The terahertz frequency lies between the microwave and infrared on the electromagnetic spectrum, ranging from 0.1 – 10 THz [1]. Due to numerous applications in the medical field [2], biosensing and chemical sensing [3, 4], biotechnology, security, imaging, and telecommunications [5, 6], it has gained significant attention from researchers in the last decade [7]. The emerging industry of PCF, also known as micro-structured fibres, has been introduced in Terahertz wave transmission due to various applications of these combinations. Different types of PCF cores, such as solid, hollow, and porous, can be designed to minimise material loss and confinement loss [8]. SC PCF works on the principle of total internal reflection (TIR), where the core is filled with a dielectric material, and the cladding has air holes with a lower refractive index [9, 10].

In the last decade, multiple articles on photonic crystal fibre in terahertz regime have been published for seeking low effective material loss (EML), confinement loss and highly effective mode area (EMA) in the core. In 2018, Islam et al. [11] designed an elliptical array-shaped rectangular PCF and culminated EML, confinement loss, power

fraction, and effective mode area of $0.06 cm^{-1}$, $5.45 \times 10^{-13} cm^{-1}$, 43 %, and $1.20 \times 10^{-7} m^2$ at 1 THz. However, they did not calculate an important V-parameter and failed to increase the frequency region. In 2019, Zhang et al. [12] proposed the porous core PCF. They evaluated EML, confinement loss, core power fraction, and effective mode area of $0.08 cm^{-1}$, $3.2 \times 10^{-13} cm^{-1}$, 57 %, and $1.20 \times 10^{-7} m^2$. In the following year, Abdullah-Al-Shafi et al. [13] suggested octagonal core PCF and calculated confinement loss, effective mode area, and core power fraction of $2.28 \times 10^{-16} cm^{-1}$, $1.49 \times 10^{-7} m^2$, and 77%. In 2021, Eid et al. [14] brought hollow-core PCF using which they calculated confinement loss, EML, NA, effective mode area, and V-parameter of $3.80 \times 10^{-13} cm^{-1}$, $1.5 \times 10^{-2} cm^{-1}$, 0.50, $5.0 \times 10^{-8} m^2$, and 3.00. In the same year, Jibon et al. [15] in the Optical Society of Japan published a porous core PCF. They calculated EML, confinement loss, core power fraction, effective mode area, V-parameter, and NA of $5.0 \times 10^{-2} cm^{-1}$, $8.01 \times 10^{-7} cm^{-1}$, 55 %, $1.5 \times 10^{-6} m^2$, 4.5, and 0.37.

In this paper, a fundamental mode SW – PCF has been proposed, and to check its reliability, various parameters such as confinement loss, EML, effective

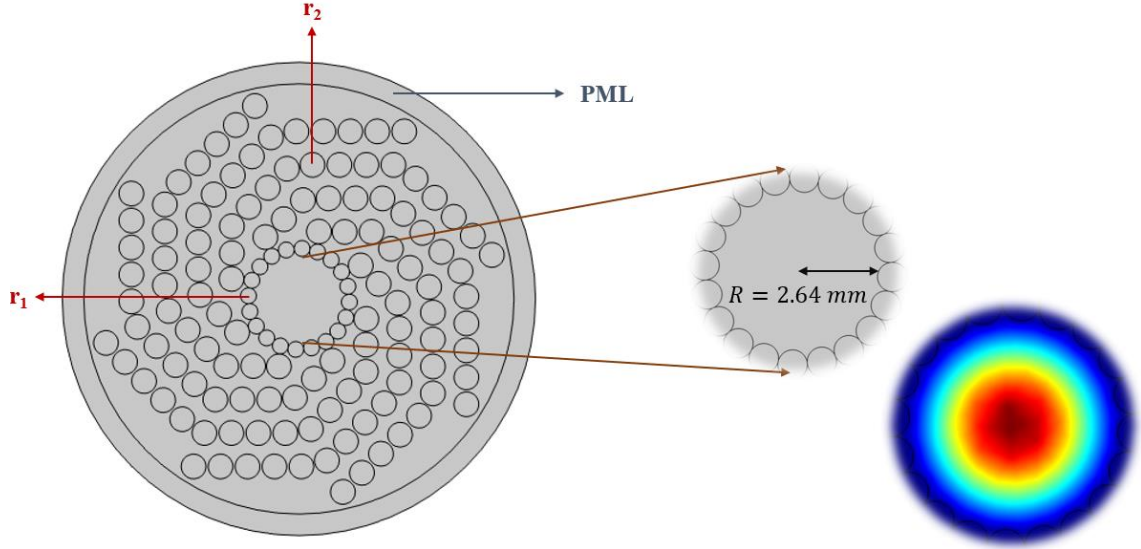


Fig. 1. Cross-sectional view of the SW PCF with the fundamental mode at 1 THz.

mode area, nonlinearity coefficient, which is ignored by researchers many times, numerical aperture (NA), core power fraction, and V-parameter have been evaluated.

2. Proposed design

The schematic cross-sectional view of the proposed SW – PCF is shown in Fig. 1 with proper parameters and core intensity. In the cladding region, the air holes are arranged in the spider web manner that can be formed by rotating a triangular structure of air holes at an angle of $\theta_n = \frac{360n}{8}$, where $n = 1, 2, 3, 4, 5, 6, \text{ and } 7$. The structure turns into a spider web arrangement by

placing the centralised air hole some distance away. In addition, air holes surrounded the core region arranged in a form that approximates it a circular core. In cladding, air holes nearer to the core have a radius of $r_1 = 213 \mu\text{m}$, and the rest has a radius of $r_2 = 332.5 \mu\text{m}$, with the air filling fraction (AFF) of 0.45 and 0.7, respectively. The fused silica is a core material used in this design because of its broad transparent transmission range, which is stretched from the ultraviolet to infrared range [16]. The perfectly matched layer attached to the fibre is used to estimate losses.

3. Numerical analysis

To evaluate the optical characterisation of the proposed SW – PCF design, FEM-based computational electrodynamics is used in COMSOL Multiphysics Software. Effective mode index and losses in PML region are essential to characterise any PCF design. The more the radiation is confined

in the core-cladding region, the better the PCF. The mode at a particular frequency consists of two factors, one is the real part of the $Re(n_{eff})$ which can be used to plot effective mode index, and another is the imaginary part of the $Im(n_{eff})$ from which confinement loss is evaluated. The confinement loss is estimated using the following equation [17]:

$$L = 8.686k_0 Im(n_{eff}) \times 10^{-2} \quad (1)$$

where $k_0 = \frac{2\pi\nu}{c}$, k_0 is the wave number; ν is the frequency of radiation used, and c is the speed of light in the free space. The proposed PCF has been formed using the super-fine transparent fused silica. However, at higher frequencies, these materials can absorb some radiation which comes as material loss or EML. It can be calculated using the following [18]:

$$\alpha_{eff} = \sqrt{\frac{\epsilon_0 \int_{mat} n_{mat} \alpha_{mat} |E|^2 dA}{u_0 2|\int_{all} S_z dA|}} \quad (2)$$

where α_{mat} is the bulk material absorption loss and S_z is the Poynting's vector. The effective mode area (A_{eff}) of the fundamental mode can be evaluated [19]:

$$A_{eff} = \frac{[\int I(r) dr]^2}{[\int I^2(r) dr]} \quad (3)$$

using the A_{eff} , nonlinearity coefficient (γ) and numerical aperture (NA) can also be evaluated that talk about the acceptance or emission of radiation by the core [20, 21],

$$\gamma = \frac{2\pi n_2}{\lambda A_{eff}} = \frac{2\pi v n_2}{c A_{eff}} \quad (4)$$

$$NA = \frac{1}{\sqrt{1 + \frac{\pi A_{eff} v^2}{c^2}}} \quad (5)$$

To know the confined power inside the core of the fibre, power fraction needs to be calculated which is [22]:

$$P = \frac{\int_i S_z dA}{\int_{All} S_z dA'} \times 100 \% \quad (6)$$

In the end, mode parameter of the fibre is examined. The V-parameter can be estimated using the following [23]:

$$V = \frac{2\pi r v}{c} \sqrt{n_{co}^2 - n_{cl}^2} \quad (7)$$

where r is the radius of the core, n_{co} and n_{cl} are effective refractive index of core and cladding, respectively.

4. Simulation results

In the proposed design, initially, the PML is taken as the 10% part of the whole PCF, which is used to estimate the EML and confinement losses of the fibre. Figure 2 depicts the confinement loss with terahertz wave transmission frequency variation. The light is confined tightly in the core region, due to which a negligible amount of confinement loss is reported. At 1 THz, the confinement loss is brought to $6.22 \times 10^{-17} \text{ cm}^{-1}$. It reaches the maximum value of $8.35 \times 10^{-16} \text{ cm}^{-1}$, which is the lowest among the previous [11–15] results.

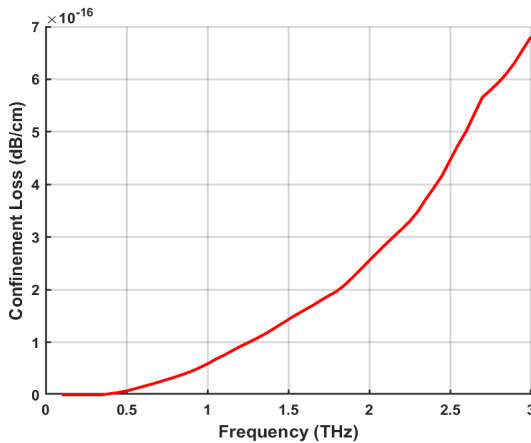


Fig. 2. Confinement loss as a function of frequency.

In Fig. 3, the EML of the fused silica material with the variation of frequency has been evaluated.

At 1 THz, it is reported $1.99 \times 10^{-2} \text{ cm}^{-1}$. The material loss is said to reach the value of bulk material absorption loss (α_{mat}) for fused silica.

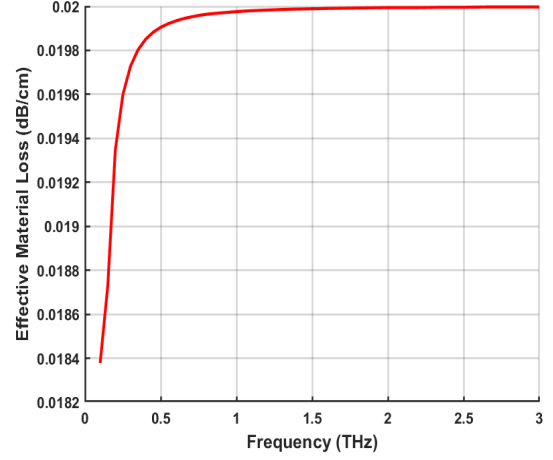


Fig. 3. Effective material loss as a function of frequency.

Figure 4 shows the effective mode area with the variation of frequency. At 1 THz, effective mode area has the most significant value of $1.08 \times 10^{-5} \text{ m}^2$ that reaches to the minimum value of $1.06 \times 10^{-5} \text{ m}^2$ at 3 THz frequency. The large effective mode area is crucial for a fibre for a huge power transmission [24]. Corresponding to effective mode area, the nonlinearity coefficient varies inversely, which is shown in Fig. 5, at 1 THz, nonlinearity coefficient has the minimum value of $2.03 \times 10^{-9} \text{ rad/W.m}$.

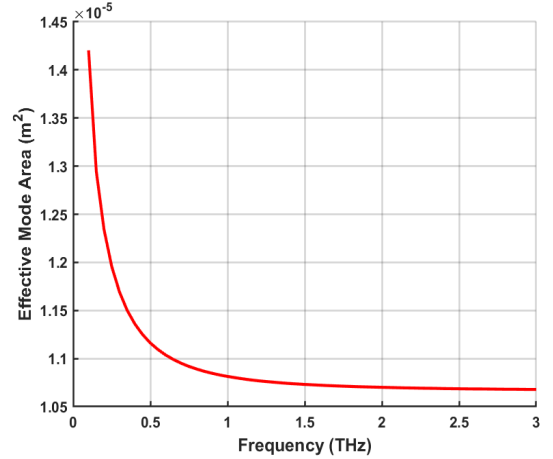


Fig. 4. Effective mode area as a function of frequency.

The NA in a fibre represents the radiation acceptance or emission through the PCF. Figure 6 illustrates the NA varying with the frequency. The higher value of NA is reported at 0.1 THz of 0.41, which is a threshold value for fused silica-based fibres.

Table 3. Performance comparison of the proposed design to existing PCF designs [11-15].

Ref.	$EML (cm^{-1})$	$L (cm^{-1})$	$A_{eff}(m^2)$	$\gamma(rad/W.m)$	NA	$Power \%$
[11]	6.0×10^{-2}	5.45×10^{-13}	1.20×10^{-7}	-	-	44
[12]	8.0×10^{-2}	3.20×10^{-13}	1.20×10^{-7}	-	-	57
[13]	-	2.28×10^{-16}	1.49×10^{-7}	-	-	77
[14]	1.5×10^{-2}	3.80×10^{-13}	5.00×10^{-8}	-	0.50	-
[15]	5.0×10^{-2}	8.01×10^{-7}	1.50×10^{-6}	-	0.37	55
This work	1.99×10^{-2}	6.22×10^{-17}	1.08×10^{-5}	2.03×10^{-9}	0.41	99

The NA in a fibre represents the radiation acceptance or emission through the PCF. Figure 6 illustrates the NA varying with the frequency. The higher value of NA is reported at 0.1 THz of 0.41, which is a threshold value for fused silica-based fibres.

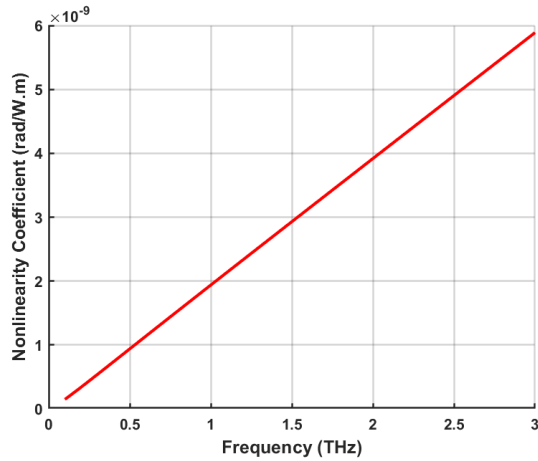


Fig. 5. Nonlinearity coefficient as a function of frequency.

In Figure 7, the higher core power fraction in the solid core PCF has been reported. Because of the tightly packed core with air holes, most radiation is confined to the core region; the power fraction is 99 % at 1 THz frequency. The V-parameter, the mode parameter of the fibre, is reported as low as 0.27. Figure 8 shows the behaviour of the V-parameter with the frequency.

Table – 1 shows the comparison between existing results and results that are calculated in this work.

5. Conclusion

A newly formed SW – PCF has been designed and simulated various optical parameters. Simulated

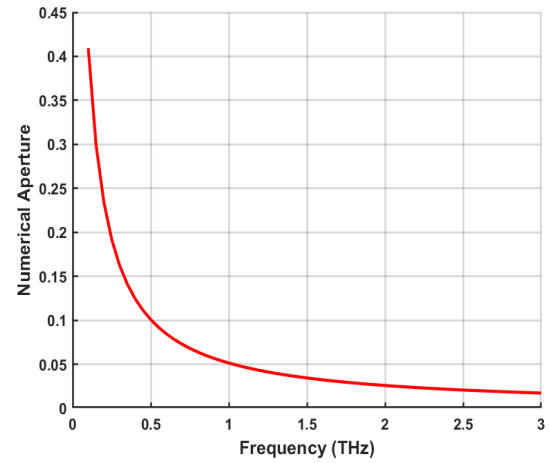


Fig. 6. Numerical aperture as a function of frequency.

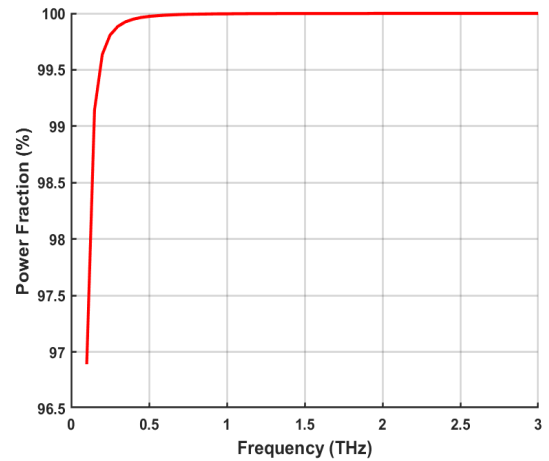


Fig. 7. Power fraction as a function of frequency.

results have shown low confinement loss and EML of $6.22 \times 10^{-17} dB/cm$ and $1.99 \times 10^{-2} dB/cm$, respectively. Moreover, from the V-parameter, the proposed structure exhibits fundamental mode properties; and the higher effective mode area, core

power fraction, and NA can attain in the broad range from 0.1 to 3.0 THz of terahertz radiation. This fibre can, indeed, be used in broadband transmission, sensing, and other applications of terahertz.

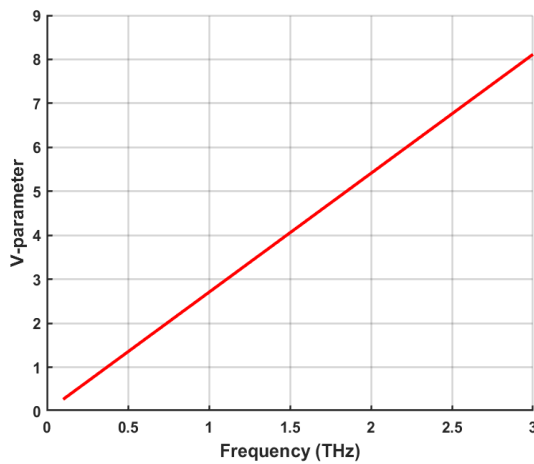


Fig. 8. V-parameter as a function of frequency.

Acknowledgement

This work was supported by the Delhi Technological University, Bawana Road, New Delhi, Delhi 110042, India.

References

1. Wang B, Jia C, Yang J, Di Z, Yao J, Zhang J. Highly birefringent, low flattened dispersion photonic crystal fiber in the terahertz region. *IEEE Photonics Journal*. 2021 Feb 8;13(2):1-0.
2. Zaytsev KI, Kudrin KG, Koroleva SA, Fokina IN, Volodarskaya SI, Novitskaya EV, Perov AN, Karasik VE, Yurchenko SO. Medical diagnostics using terahertz pulsed spectroscopy. *InJournal of Physics: Conference Series* 2014 Mar 18 (Vol. 486, No. 1, p. 012014). IOP Publishing.
3. Rifat AA, Mahdiraji GA, Sua YM, Shee YG, Ahmed R, Chow DM, Adikan FM. Surface plasmon resonance photonic crystal fiber biosensor: a practical sensing approach. *IEEE Photonics Technology Letters*. 2015 May 13;27(15):1628-31.
4. Arif MF, Asaduzzaman S, Biddut MJ, Ahmed K. Design and optimization of highly sensitive photonic crystal fiber with low confinement loss for ethanol detection. *Int. J. Technol.* 2016 Jan 1;6:1068-76.
5. Sen S, Abdullah-Al-Shafi M, Sikder AS, Hossain MS, Azad MM. Zeonex based decagonal photonic crystal fiber (D-PCF) in the terahertz (THz) band for chemical sensing applications. *Sensing and Bio-Sensing Research*. 2021 Feb 1;31:100393.
6. Hasanuzzaman GK, Rana S, Habib MS. A novel low loss, highly birefringent photonic crystal fiber in THz regime. *IEEE Photonics Technology Letters*. 2016 Jan 12;28(8):899-902.
7. Wu Z, Shi Z, Xia H, Zhou X, Deng Q, Huang J, Jiang X, Wu W. Design of highly birefringent and low-loss oligoporous-core THz photonic crystal fiber with single circular air-hole unit. *IEEE Photonics Journal*. 2016 Dec 1;8(6):1-1.
8. Abdullah-Al-Shafi M, Akter N, Sen S, Hossain MS. Design and performance analysis of background material of zeonex based high core power fraction and extremely low effective material loss of photonic crystal fiber in the terahertz (THz) wave pulse for many types of communication areas. *Optik*. 2021 Oct 1;243:167519.
9. Ademgil H. Highly sensitive octagonal photonic crystal fiber based sensor. *Optik*. 2014 Oct 1;125(20):6274-8.
10. Ahmed K, Morshed M. Design and numerical analysis of microstructured-core octagonal photonic crystal fiber for sensing applications. *Sensing and Bio-Sensing Research*. 2016 Mar 1;7:1-6.
11. Islam MS, Sultana J, Dinovitsier A, Faisal M, Islam MR, Ng BW, Abbott D. Zeonex-based asymmetrical terahertz photonic crystal fiber for multichannel communication and polarization maintaining applications. *Applied optics*. 2018 Feb 1;57(4):666-72.
12. Zhang Y, Xue L, Qiao D, Guang Z. Porous photonic-crystal fiber with near-zero ultra-flattened dispersion and high birefringence for polarization-maintaining terahertz transmission. *Optik*. 2020 Apr 1;207:163817.
13. Abdullah-Al-Shafi M, Sen S. Design and analysis of a chemical sensing octagonal photonic crystal fiber (O-PCF) based optical sensor with high relative sensitivity for terahertz (THz) regime. *Sensing and Bio-Sensing Research*. 2020 Aug 1;29:100372.
14. Eid MM, Habib MA, Anower MS, Rashed AN. Hollow core photonic crystal fiber (PCF)-Based optical sensor for blood component detection in terahertz spectrum. *Brazilian Journal of Physics*. 2021 Aug;51:1017-25.
15. Jibon RH, Bulbul AA, Nahid AA, Faragallah OS, Baz M, Eid MM, Rashed AN. Design and numerical analysis of a photonic crystal fiber (PCF)-based flattened dispersion THz waveguide. *Optical Review*. 2021 Oct;28(5):564-72.
16. Tran D, Sigel G, Bendow B. Heavy metal fluoride glasses and fibers: a review. *Journal of Lightwave Technology*. 1984 Oct;2(5):566-86.
17. Li S, Liu H, Huang N, Sun Q. Broadband high birefringence and low dispersion terahertz photonic

- crystal fiber. *Journal of Optics*. 2014 Sep 23;16(10):105102.
18. Islam MS, Sultana J, Rifat AA, Dinovitser A, Ng BW, Abbott D. Terahertz sensing in a hollow core photonic crystal fiber. *IEEE Sensors Journal*. 2018 Mar 26;18(10):4073-80.
19. Kaijage SF, Ouyang Z, Jin X. Porous-core photonic crystal fiber for low loss terahertz wave guiding. *IEEE Photonics Technology Letters*. 2013 Jun 6;25(15):1454-7.
20. Agbemabiese PA, Akowuah EK. Numerical analysis of photonic crystal fiber of ultra-high birefringence and high nonlinearity. *Scientific Reports*. 2020 Dec 3;10(1):1-2.
21. Islam MS, Sultana J, Ahmed K, Islam MR, Dinovitser A, Ng BW, Abbott D. A novel approach for spectroscopic chemical identification using photonic crystal fiber in the terahertz regime. *IEEE Sensors Journal*. 2017 Nov 20;18(2):575-82.
22. Islam MS, Sultana J, Dinovitser A, Ng BW, Abbott D. A novel Zeonex based oligoporous-core photonic crystal fiber for polarization preserving terahertz applications. *Optics Communications*. 2018 Apr 15;413:242-8.
23. Wu Z, Zhou X, Xia H, Shi Z, Huang J, Jiang X, Wu W. Low-loss polarization-maintaining THz photonic crystal fiber with a triple-hole core. *Applied Optics*. 2017 Mar 10;56(8):2288-93.
24. Ahmed K, Chowdhury S, Paul BK, Islam MS, Sen S, Islam MI, Asaduzzaman S. Ultrahigh birefringence, ultralow material loss porous core single-mode fiber for terahertz wave guidance. *Applied optics*. 2017 Apr 20;56(12):3477-83.